frontiers | Frontiers in Nanotechnology

TYPE Review
PUBLISHED 03 June 2025
DOI 10.3389/fnano.2025.1603334

OPEN ACCESS

EDITED BY
Weijing Yang,
Zhengzhou University, China

REVIEWED BY
Hongwu Sun,
Third Military Medical University, China
Soubantika Palchoudhury,
University of Dayton, United States

*CORRESPONDENCE
Yan Luo,
yanluo2018@cqu.edu.cn

RECEIVED 12 April 2025
ACCEPTED 26 May 2025
PUBLISHED 03 June 2025

CITATION
Luo Y (2025) Radiobiological perspective on metrics for quantifying dose enhancement effects of High-Z nanoparticles.
Front. Nanotechnol. 7:1603334.
doi: 10.3389/fnano.2025.1603334

Radiobiological perspective on metrics for quantifying dose enhancement effects of High-Z nanoparticles

Yan Luo*

Radiation Oncology Center, Chongqing University Cancer Hospital, Chongqing, China

High atomic number (high-Z) metal nanoparticles (NPs) have emerged as transformative radiosensitizers in cancer radiotherapy, offering the potential to amplify tumor-specific radiation effects while sparing healthy tissues. However, the clinical translation of these NPs is hindered by inconsistent methodologies for quantifying dose enhancement and a limited understanding of how biological complexity influences therapeutic outcomes. This review systematically evaluates current metrics for assessing high-Z NP-mediated radiosensitization, including physical dose enhancement factors (DEF), sensitizer enhancement ratios (SER), survival fraction (SF), and DNA damage biomarkers. We critically analyze the interplay between NP properties, radiation parameters, and tumor microenvironment (TME) dynamics, emphasizing how hypoxia, immune suppression, and stromal barriers modulate therapeutic efficacy. A key innovation is the proposal of a multidimensional Radiosensitization Index (RSI), integrating physical dose deposition, reactive oxygen species (ROS) kinetics, DNA repair inhibition, immune reprogramming, and clinical endpoints. We further highlight translational challenges such as NP toxicity, batch-to-batch variability, and the discordance between *in vitro* and *in vivo* models, underscoring the need for standardized protocols and advanced 3D/organoid platforms. By bridging radiobiology, nanotechnology, and clinical practice, this work provides a roadmap for optimizing NP-enhanced radiotherapy and accelerating its integration into precision oncology.

KEYWORDS

high-Z nanoparticles, radiosensitization, dose enhancement, radiation therapy, nanomedicine

1 Introduction

Cancer remains a global health crisis, with 20% of individuals diagnosed during their lifetime (Bray et al., 2024). As the second leading cause of mortality worldwide, cancer resulted in over 9.7 million deaths in 2022, with projections suggesting a rise to 13 million deaths by 2030 (Bray et al., 2024). While cancer treatments like surgery, chemotherapy, targeted therapy, and immunotherapy have advanced significantly, radiation therapy (RT) continues to play a central role (Schaue and McBride, 2015; Chen et al., 2021). Clinically, RT is used in 60%–70% of cancer cases (Baumann et al., 2016). Technological advancements in external beam radiation therapy (EBRT), particularly intensity-modulated radiation therapy (IMRT) and volumetric modulated arc therapy (VMAT), have enhanced treatment precision while minimizing damage to the healthy tissues (Pan et al., 2024;

Chun et al., 2024). However, RT faces two major limitations. Firstly, collateral damage to healthy tissues restricts maximum tumor dose delivery (Verginadis et al., 2025). Secondly, radioresistant tumors require doses exceeding normal tissue tolerance (Zhang et al., 2025). These challenges drive the development of radiosensitizers to amplify tumor-specific radiation effects while sparing healthy tissues.

Since the landmark study on gold nanoparticles as radiosensitizers in 2004 (Kreipl et al., 2009), high atomic number (high-Z) nanoparticles (NPs), such as gold (Au), gadolinium (Gd), and bismuth (Bi), have emerged as promising radiosensitizers (Chen et al., 2020; Schuemann et al., 2020). These NPs work through three key mechanisms: 1) Physical enhancement: high-Z NPs increase localized energy deposition via photoelectric and Auger effects (Zhu et al., 2025a; Liu et al., 2024). 2) Chemical enhancement: NPs catalyze reactive oxygen species (ROS) generation, exacerbating radiation-induced DNA damage (Tan et al., 2025; Wang et al., 2024b). 3) Biological enhancement: NPs disrupt DNA repair pathways, prolong cell cycle arrest, and amplify bystander effects (Fan et al., 2025; Morris et al., 2025; Wang et al., 2024a). Despite preclinical success, the clinical translation remains limited. Major translation barriers include difficulties in mass-producing precisely engineered nanoparticles and critical knowledge gaps in the understanding of nanoparticle design, biological interactions, and quantification methodologies. Specifically, the inadequate comprehension of radiotherapy enhancement mechanisms and the quantification of dose enhancement hampers the development of optimal candidate materials (Babaye Abdollahi et al., 2021; Tan et al., 2025; Gerken et al., 2024). This review systematically examines current knowledge on high-Z NP-mediated radioenhancement mechanisms and critically evaluates metrics for quantifying their effects, aiming to bridge gaps between radiobiology, nanotechnology, and clinical practice.

2 Challenges in modern radiotherapy: Progress and critical perspective

Modern radiotherapy has evolved significantly with technological advancements, yet fundamental challenges persist. Below, we analyze these challenges through both clinical limitations and research opportunities, integrating critical perspectives to highlight unresolved problems.

2.1 Physical limitations of conventional RT techniques: beyond dose conformity

Radiotherapy traces its origins back to the late 19th century with the discovery of X-rays (Pfeiffer et al., 2020). Early two-dimensional (2D) planning progressed to three-dimensional (3D) conformal techniques that better protected healthy tissues. Today, IMRT is the standard for EBRT, using adjustable beam intensities to precisely target tumors. Other advances like VMAT, Image-Guided Radiation Therapy (IGRT), and Stereotactic Body Radiation Therapy (SBRT) further improve the precision of photon beam therapy (Mancuso et al., 2012; Franzone et al., 2016; Teoh et al., 2011). Proton therapy adds another dimension through the Bragg peak effect, which concentrates radiation at tumor sites while sparing deeper healthy tissues (Yan et al., 2023; Huff, 2007). While IMRT and proton therapy have improved dose conformity, their limitations are multifaceted. Photon therapy with low-energy beams (6–20 MeV) risks damaging tissues beyond the tumor due to exit doses (Galloway et al., 2012). High-energy photons (>20 MeV) reduce skin exposure but introduce neutron contamination (0.1–0.5 Sv/Gy for 18 MeV linear accelerators), complicating long-term risk assessments (Paganetti et al., 2021). Proton therapy minimize exit doses but faces variable biological effectiveness (RBE range, 1.05–1.7), leading to unpredictable tumor coverage (Traneus and Oden, 2019). Moreover, proton facilities cost over $100 million, making them accessible to <1% of patients globally (Yan et al., 2023).

2.2 Tumor heterogeneity and radioresistance: molecular complexity and NP-driven solutions

The efficacy of radiotherapy is often limited by the phenomenon of radioresistance, which refers to a tumor's ability to withstand radiation exposure. Extensive research has been conducted to uncover the mechanisms underlying cancer radioresistance. Generally, tumor radioresistance stems from hypoxia, cancer stem cells (CSCs), the tumor microenvironment, enhanced DNA repair, and various signaling pathways (Busato et al., 2022; Deng et al., 2023). Hypoxic regions (pO_2 < 10 mmHg) exhibit 3-fold higher radioresistance, prompting the use of catalytic NPs like MnO_2 to convert tumor H_2O_2into O_2, boosting oxygenation significantly in preclinical models (Pi et al., 2023). However, current NP designs predominantly target bulk tumor cells, neglecting CSC niches that cause recurrence. For example, glioblastoma CSCs ($CD44^+/CD133^+$) show 2-fold higher post-RT survival (Tsai et al., 2021), but AuNPs conjugated with DNA fragments reduce their survival significantly, highlighting the potential of CSCs-targeting strategies (Kunoh et al., 2019). Future NPs should incorporate hypoxia-responsive drug release and CSC-specific ligands to address these layered resistance mechanisms. Additionally, precision medicine based on the individual genetic and molecular characteristics is being explored as a potential approach to combat radioresistance.

2.3 Normal tissue toxicity: balancing efficacy and safety

Theoretically, tumors and normal tissues exhibit differential sensitivity to radiation. The radiosensitivity of highly metabolic or functionally active tumor cells usually surpasses that of adjacent normal tissues (Liu et al., 2025; Alkotub et al., 2025). The objective of radiotherapy is to maximize the irradiation dose to the tumor while minimizing exposure to surrounding healthy tissues. Therefore, balancing efficacy and safety remains critical, as healthy tissue toxicity constrains dose escalation. Experiments demonstrate that tumor-specific accumulation of NPs can achieve favorable tumor-to-normal tissue concentration ratios to minimize collateral damage (Reda et al., 2020). The size, shape, and surface functionalization of NPs critically influence biodistribution and

clearance. As reported, smaller AuNPs with diameter of 1.9 nm exhibit efficient renal clearance and low systemic toxicity in murine models (Reda et al., 2020). Additionally, localized intratumoral injection of NPs further reduces systemic exposure and associated normal tissue risks (Bai et al., 2020). While high-Z NPs enhance radiation-induced DNA damage and ROS production in tumors, their catalytic activity and prolonged retention in healthy tissues could exacerbate normal cell toxicity (Gerken et al., 2023). Promising strategies include combining NPs with tumor-specific drugs to suppress DNA repair pathways, or designing biodegradable NPs to boost radiation effects while ensuring rapid metabolic clearance. Future research should prioritize NP design innovations, such as size-tunable architectures, tumor microenvironment-responsive coatings, and hybrid systems, which could maximize tumor-selective radiosensitization while mitigating collateral damage to normal tissues. For instance, hyaluronidase/ROS cascade-responsive systems demonstrate size/charge switching from ~150 nm to sub-50 nm particles upon entering acidic tumor regions, enabling deep tissue penetration while maintaining circulatory stability (Shi et al., 2024b), while gelatin-based platforms achieve tumor-selective size transitions through pH/enzyme dual-responsive mechanisms (Khandal et al., 2025). Hybrid designs integrating metal cores with stimuli-responsive polymer coatings liked HA-modified systems may optimize both radiation dose enhancement and biological targeting precision, as demonstrated in tumor-penetrating nanocomplexes that leverage size modulation to overcome stromal barriers (Khandal et al., 2025; Shi et al., 2024b). These innovations align with emerging strategies that couple physical radiosensitization with microenvironmental adaptation (Mansouri et al., 2023; Fu et al., 2025).

2.4 Technological and biological synergies: a call for integration

Emerging technologies like FLASH-RT and MRI-guided RT offer synergistic potential. FLASH-RT's ultra-high dose rates (40 Gy/s) protect normal tissues but require NPs stable under extreme conditions (Shen et al., 2024). Preliminary data show TaNPs enhance FLASH efficacy without compromising tissue protection (Meng et al., 2023). MRI-guided RT with GdNPs for real-time tumor tracking demonstrates superior antitumor performance without systemic toxicity or long-term side effects (Sun et al., 2020). However, progress is slowed by insufficient collaboration between radiation oncologists, nanotechnologists, and biologists. Joint efforts should focus on developing NP-RT platforms validated in both preclinical and clinical settings. Future NPs need smart features like pH/ROS-activated drug release and designs meeting safety regulations for immune impacts and long-term toxicity. For instance, pH-responsive hybrid micelles combining inorganic NPs with pH-sensitive amphiphiles enable tumor-acidic-triggered drug release, minimizing off-target toxicity while leveraging high-Z elements (Au, Bi) for localized radiation dose amplification (Moloudi et al., 2023; Gimeno-Ferrero et al., 2024). Recent advancements in pH-stabilized Prussian blue-based nanocomposites further illustrate how acid-triggered structural transformations synchronize drug release with radiosensitization, addressing dynamic TME challenges (Shi et al., 2024a). Additionally, lipid NPs functionalized with pH-responsive bicontinuous cubic phases achieve tumor-selective drug delivery, exemplifying translational designs that align with safety regulations for immune compatibility (Rajesh et al., 2022). These innovations highlight the dual utility of pH-activated mechanisms in optimizing high-Z nanodrugs for precision radiotherapy.

3 Mechanism of High-Z NP-mediated radioenhancement

3.1 Physical dose enhancement: from simulations to biological impact

High-Z NPs enhance radiotherapy through physical, chemical, and biological mechanisms, each contributing uniquely to dose enhancement (Figure 1). Under X-ray irradiation, high-Z NPs can trigger a series of physical process, including the Photoelectric effect, Auger effect, and Compton scattering (Chen et al., 2019). These interactions lead to the generation of secondary electrons, X-rays, and fluorescent light, increasing energy deposition in tumors. Both simulations and experimental studies confirm that the dose enhanced factor (DEF) depends on radiation energy. The strongest effects occur at kilovoltage (KeV) X-ray energies (50–300 KeV), where the photoelectric effect dominates (Schuemann et al., 2016; Her et al., 2017). For example, 15 nm AuNPs combined with 100 KeV X-rays achieved DEF values exceeding 2.0 in breast cancer cells, whereas megavoltage (MeV) beams yielded significantly lower DEF (1.2–1.5) due to reduced photoelectric interactions (Tudda et al., 2022). Additionally, the size and concentration of AuNPs further modulate DEF, with smaller particles and intratumoral accumulation showing superior sensitization in preclinical models (Zhang et al., 2012). However, physical effects alone cannot fully explain *in vivo* therapeutic gains, requiring integration with chemical and biological mechanisms.

3.2 Chemical ROS amplification: mechanisms and quantification

High-Z NPs enhance radiation by catalytically increasing ROS generation. High-Z NPs amplify water radiolysis to produce hydroxyl radicals (·OH), superoxide anions (O_2^-), and hydrogen peroxide (H_2O_2) (Gerken et al., 2023). AuNPs, for example, produce low but biologically significant ROS levels detected by FLIM-ROX, a sensitive imaging method capable of tracking ROS in living systems (Balke et al., 2018). This ROS amplification disrupts redox homeostasis, exacerbating DNA damage, mitochondrial dysfunction, and apoptosis, thereby sensitizing cancer cells to radiation (Yadav et al., 2024; Yang et al., 2025). However, ROS quantification remains challenging due to methodological limitations. Common probes like H_2DCF-DA suffer from artifacts such as auto-oxidation, photo-bleaching, and poor specificity, leading to overestimated ROS levels (Balke et al., 2018). Electron spin resonance (ESR) detects radicals specifically but lacks sensitivity in biological systems and requires complex sample preparation,

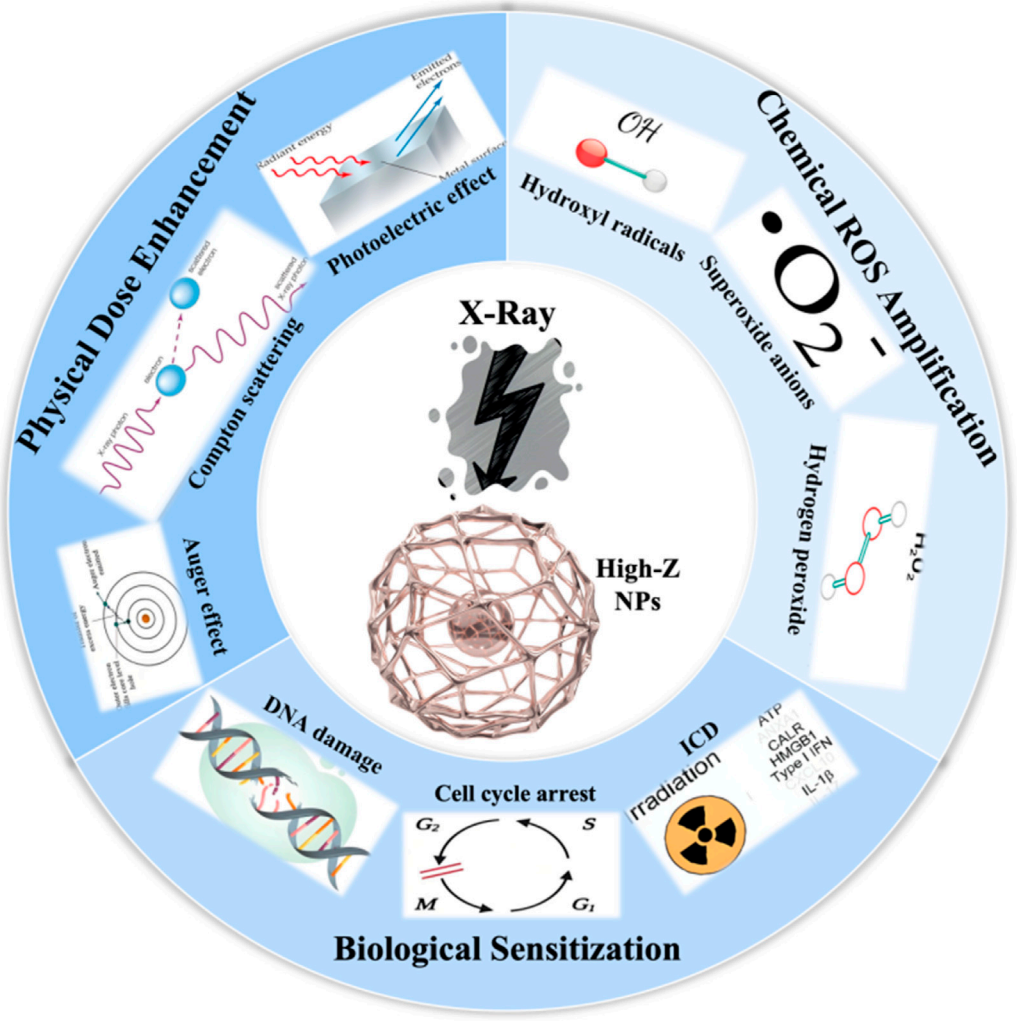

FIGURE 1
Scheme of the mechanism of high-Z NP-mediated radioenhancement.

limiting its applicability in dynamic cellular environments (Yang et al., 2025). Advanced tools like multiphoton FLIM-ROX enable high-resolution, real-time ROS mapping with minimal interference (Balke et al., 2018). However, standardized protocols for ROS quantification are still needed, with emerging techniques like surface-enhanced Raman spectroscopy (SERS) improving accuracy and reproducibility (Chen et al., 2025). SERS offers distinct advantages for ROS quantification, including ultrahigh sensitivity for detecting transient ROS at low concentrations in real time (Yang et al., 2025), and the ability to achieve spatially resolved monitoring of ROS dynamics within subcellular compartments through localized plasmonic enhancement (Ding et al., 2025b; Chen et al., 2022). Unlike conventional methods, SERS minimizes interference from complex biological matrices by leveraging molecular fingerprint specificity and enzyme-mimicking signal amplification strategies (Wu et al., 2024), while recent advances in substrate engineering have significantly improved reproducibility for quantitative analysis (Kao et al., 2025; Cai et al., 2023). These features position SERS as a transformative tool for standardizing ROS measurements in radiobiological studies.

3.3 Biological sensitization: beyond physical interactions

The biological mechanisms underpinning high-Z NPs-mediated radiosensitization extend far beyond physical and chemical effects. Emerging evidence highlights their ability to disrupt DNA repair pathways, modulate cell cycle progression, induce bystander effects, and reprogram the tumor immune microenvironment (Yuan et al., 2024; Das, 2025; Xu et al., 2024). For example, platinum-based NPs (PtNPs) have been shown to inhibit BRCA1-mediated DNA repair, worsening radiation-induced DNA damage (Hullo et al., 2021). Gadolinium-carbon dots (Gd@Cdots) trap cells in the radiation-sensitive G2/M phase, amplifying chromosomal fragmentation and mitotic catastrophe (Lee et al., 2021). Intriguingly, AuNPs can trigger bystander effects through the release of mitochondrial ROS and pro-apoptotic factors, sensitizing neighboring cells without direct NP uptake (Choi et al., 2018). Emerging evidence also implicates significance of immune modulation. Iridium (Ir)-based nanoplatforms polarize tumor-associated macrophages toward the pro-inflammatory M1 phenotype and promote

dendritic cell maturation, fostering systemic antitumor immunity alongside localized radiosensitization (Zou et al., 2023). Moreover, combinatorial strategies utilizing high-Z NPs with immunogenic cell death (ICD) inducers enhance antigen presentation and T-cell infiltration, overcoming radioresistance in immunologically "cold" tumors (Zhen et al., 2023). While biological sensitization offers a multidimensional approach to radiotherapy enhancement, its clinical translation requires addressing NP heterogeneity in cellular uptake and off-target immune activation.

The conventional "three-phase" model (physical-chemical-biological) fails to capture systemic effects like immune modulation or bystander effects. A "systems radiobiology" approach integrating multi-omics is needed to map NP-induced molecular networks (Karapiperis et al., 2021). Furthermore, while most research focuses on photon beams, NP interactions with protons or carbon ions remain under explored. Monte Carlo simulations suggest Au, Pt, Gd, and Fe NPs enhance proton energy deposition by 14–27% at 5–50 MeV (Martinez-Rovira and Prezado, 2015; McKinnon et al., 2016), but experimental validation is lacking. To translate these mechanisms into clinical practice, NP formulations should be co-engineered with imaging tracers for real-time monitoring of tumor distribution and dose enhancement, which is a critical step toward personalized radiotherapy.

3.4 Comparative analysis of High-Z NPs: surface modification, morphology, and size-dependent effects

The radiosensitization efficacy of high-Z NPs such as Au, Gd, and Bi is intrinsically linked to their physicochemical properties, including surface modifications, morphology, and size. GNPs have been extensively studied due to their tunable size (2–100 nm) and morphology-dependent optical properties, which enable precise control over surface plasmon resonance effects (Ding et al., 2025a; Kaercher and Lear, 2025). For instance, thiolated surface functionalization enhances GNPs' biocompatibility and reduces aggregation in biological environments (Wang et al., 2025), while ATP-coated ultrasmall GNPs (2–5 nm) exhibit selective binding capabilities to biomolecular targets (Katrivas et al., 2023). The surface roughness of GNPs, influenced by aspect ratios (1:1 to 1: 10), also plays a critical role in minimizing cytotoxicity when integrated into biomedical devices (Shin et al., 2023). In contrast, Gd-based nanoparticles, such as gadolinium oxide (GdO), demonstrate unique advantages due to their paramagnetic properties and high X-ray attenuation. Surface modification with bovine serum albumin (BSA) in GdO@BSA-Au hybrid NPs not only improves colloidal stability but also synergistically enhances radiation dose deposition within tumors (Nosrati et al., 2023). Spherical Gd orthoferrite NPs with uniform surface morphology further exhibit enhanced biocompatibility and cellular uptake, as confirmed by FE-SEM and HR-TEM analyses (Guganathan et al., 2022). Bismuth oxide (BiO) NPs, on the other hand, are notable for their high photoelectric absorption cross-section. Surface functionalization with β-cyclodextrin (β-CD) improves their dispersibility and enables efficient drug loading (Alex and Mathew, 2023), while BiSe nanosheets with thiolated gold nanoclusters achieve superior surface area and charge modulation for targeted applications (Li et al., 2024). Size-dependent effects are particularly pronounced in Bi NPs, where smaller particles (<30 nm) exhibit higher radiosensitization due to increased surface-to-volume ratios (Guruswamy Pandian et al., 2025). Importantly, Monte Carlo simulations reveal that secondary electron emission peaks at distinct energies for Au (30 keV), Bi (30 keV), and Gd (60 keV), highlighting material-specific radiation enhancement mechanisms (Mansouri et al., 2024). Collectively, these findings underscore the necessity of tailoring surface chemistry, size, and morphology to optimize the therapeutic index of high-Z NPs, with GNPs excelling in tunable surface engineering, Gd NPs in multimodal imaging compatibility, and Bi NPs in high-Z-driven dose enhancement (Stergioula et al., 2023). Future research should focus on standardizing synthesis protocols to reconcile disparities in reported dose enhancement factors across studies.

4 Quantification of dose enhancement: multidimensional metrics and translational challenges

4.1 Survival fraction (SF) and mean inactivation dose (MID): from empirical models to mechanistic insights

Survival Fraction (SF) is a fundamental radiobiological parameter quantifying the proportion of cells retaining clonogenic potential after irradiation. Derived from clonogenic assays (Subiel et al., 2016), SF reflects the cumulative effects of DNA damage and repair mechanisms, serving as a critical endpoint to evaluate radiation efficacy and sensitizer performance (Figure 2). The linear-quadratic (LQ) model ($SF = \exp(-\alpha D - \beta D^2)$) distinguishes between lethal (α) and sublethal (β) damage (Hong et al., 2024; Abdollahi et al., 2024). Higher α values indicate stronger radiosensitization by increasing irreparable damage per unit dose. For example, thulium (III) oxide NPs (Tm_2O_3) combined with carboplatin reduced SF in metastatic cutaneous squamous cell carcinoma models compared to radiation alone (Perry et al., 2020). However, recent studies highlight emerging insights into the biocompatibility and toxicological profiles of TmO NPs. For instance, TmO NPs designed with varying thulium compositions demonstrated enhanced X-ray absorption and ROS generation capabilities, suggesting oxidative stress as a potential mechanism of toxicity (Zhu et al., 2025b). Additionally, critical gaps persist in understanding organ-specific accumulation and chronic exposure effects of TmO NPs, necessitating systematic *in vivo* toxicokinetic studies to bridge current knowledge limitations. Similarly, gold nanowires also suppressed SF in breast cancer models more effectively than nanospheres, likely due to higher oxidative stress and α elevation than spherical counterparts (Bai et al., 2020). Notably, TiO_2 nanotubes were shown to increase the α value while simultaneously decreasing the β value (Mirjolet et al., 2013). These findings suggest a higher α/β ratio in tumor cells treated with nanoradiosensitizers, indicating increased tumor sensitivity to ionizing radiation. Basically, most studies use a 2 Gy dose to evaluate the effectiveness of NPs *in vitro*, as it corresponds to the standard dose per fraction in conventional radiotherapy (Subiel et al., 2016). However, some studies

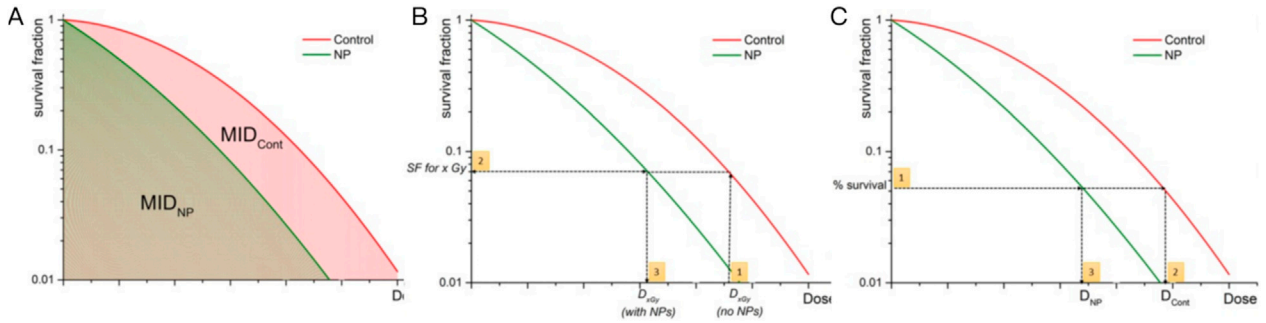

FIGURE 2
Graphical representation of quantification of NP-mediated radiation enhancement effect from clonogenic survival data. **(A)** Quantification of the radiobiological impact of NPs by calculating the ratio of MIDs. **(B)** DEF is calculated through estimation of the SF level through the following steps: (1) $D_{x\ Gy}$ (no NP) is chosen, (2) SF at $D_{x,Gy}$ (no NP) is evaluated, (3) $D_{x,Gy}$ (with NPs) is calculated). **(C)** SER is calculated as the ratio of radiation doses required to achieve the same biological effect with and without NPs. Reproduced with permission of Creative Commons Attribution 4.0 License (Subiel et al., 2016).

calculate the DEF based on survival levels using acute doses of 3 Gy (SF_3) (Coulter et al., 2012; Taggart et al., 2014), 4 Gy (SF_4) (Taggart et al., 2014; Maggiorella et al., 2012), or 8 Gy (SF_8) (Taggart et al., 2014; Maggiorella et al., 2012). Table 1 listed nanoparticle studies using survival fraction to calculate dose enhancement effect (Table 1). While SF remains a gold standard, nanoparticle off-target effects may complicate clonogenic assay results. Innovations in 3D tumor models and real-time SF monitoring could refine predictive power, bridging *in vitro* findings to clinical translation.

The mean inactivation dose (MID), calculated as the area under the SF curve, reflects the average dose required to inactivate a cell population (Figure 2A). The concept of MID was firstly introduced to assess survival curves of mammalian cells. Recent advances in high-Z NP-mediated radiosensitization used MID to quantify dose enhancing effects. For example, studies using iron oxide NPs (IONs) under proton irradiation demonstrated enhanced localized energy deposition via Coulomb nanoradiator (CNR) effects, which amplified secondary electron emission and ROS generation by 1.2 to 2.5 fold (Jeon et al., 2016). Diverging from conventional metrics, MID offers a holistic view of cellular response dynamics, particularly valuable for high-Z NPs where heterogeneous energy deposition complicates traditional models. Table 2 listed NP studies using MID to calculate dose enhancement effect (Table 2).

4.2 Dose enhancement factor (DEF) and sensitizer enhancement ratio (SER): bridging physics and biology

The dose enhancement factor (DEF), defined as the ratio of radiation dose in the presence of NPs to that without NPs (Figure 2B), primarily quantifies the physical dose amplification from the high photoelectric and Auger electron yields of high-Z materials (Chow and Jubran, 2023). In contrast, sensitizer enhancement ratio (SER), calculated as the ratio of radiation doses required to achieve the same biological effect with and without NPs (Figure 2C), incorporates both physical dose enhancement and biological interactions (Guerra et al., 2022). Studies on high-Z NPs have demonstrated significant DEF and SER values under varying irradiation conditions. For example, AuNPs exhibited a DEF of 5.7–8.1 in clinical megavoltage (MeV) beams at depths up to 30 cm (Gerken et al., 2024). Similarly, magnetic FeO@AuNPs achieved a DEF of 22.17% in cytoplasm under a magnetic field, demonstrating the role of NP targeting in enhancing local dose deposition (Mesbahi et al., 2022). However, SER values are more context-dependent. For glioblastoma cells, AuNPs achieved SER values of 1.5–1.8, while iron oxide NPs (IONPs) showed lower SER values (1.09–1.32), emphasizing the importance of NP composition and cell type (Guerra et al., 2022). Notably, coating layers and aggregation states of NPs also influence DEF and SER, as thicker coatings may attenuate secondary electron emission, while optimized surface functionalization can improve tumor retention and radiation interaction (Mansouri et al., 2023).

A critical perspective emerges from the interplay between DEF and SER. While DEF often dominates in kilovoltage (KeV) X-rays due to strong photoelectric effects, but SER gains importance in MeV beams through biological mechanisms like ROS amplification (Gerken et al., 2024). For example, Hf-based NPs achieved a SER of 1.55 at 30 cm depth under MeV beams, suggesting that biological sensitization may outweigh physical dose enhancement in deep-seated tumors (Gerken et al., 2024). However, challenges persist in translating these metrics to clinical practice. Variability in NP distribution within tumors, inconsistent DEF-SER correlations across studies, and the lack of standardized protocols for measuring these parameters hinder robust comparisons. A summary of DEF and SER used in NP studies can be found in Table 3 (Table 3).

4.3 ROS and DNA damage quantification: from probes to clinical correlations

ROS generation and DNA damage are crucial to NP-mediated radiosensitization. However, their quantification faces technical challenges. Fluorescent probes like H_2DCF-DA are widely used for ROS detection due to their accessibility and compatibility with live-cell imaging. However, limitations such as auto-

TABLE 1 Overview of Survival Fraction (SF) used in nanoparticle studies.

Enhancement factor used	NP material (size)	Radiation source	Cell line	Reference
SF_4	Au-NPs	160 KeV X-rays	DU145	Jain et al. (2011)
α, β- qualitative analysis	(1.9 nm)	6 MeV X-rays	MDA-MB-231	
		15 MeV X-rays	L132	
SF_2	Ti-NPs	MeV photons (LINAC)	SNB-19	Mirjolet et al. (2013)
α, β- qualitative analysis	(10 nm)		U87MG	
SF_2	Gd_2O_3-NPs	Cs-137	U87	Yu (2015)
SF_5	(sub-10 nm)			
SF_8				
SF	GdBN	Gamma ray, ^{60}Co irradiator	U87	Stefancikova et al. (2016)
	(3 nm)			
α, β- qualitative analysis	Au-NPs	225 KeV X-rays	MDA-MB-231	Cui et al. (2014)
	(2.7 nm)			
α, β- qualitative analysis	Au-NPs	160 KeV X-rays	MDA-MB-231	Jain et al. (2014)
	(1.9 nm)		DU145	
α, β- qualitative analysis	Au-NPs	30–100 KeV synchrotron X-rays	BAOEC	Rahman et al. (2014)
	(1.9 nm)			
SF_2	Gd based NPs	6 MeV X-rays	U87	Mowat et al. (2011)
SF_5				
SF_8				
SF_3	Gd-doped Ti NPs	250 KeV X-rays	CCL-136	Morrison et al. (2017)
	(5–20 nm)		CRL-7763	
SF_2	Au-NPs	6 MeV X-rays	U87	Kazmi et al. (2020)
	(42 nm)			
SF_2	Au-NPs	100 KeV	MDA-MB-231	Tudda et al. (2022)
	(15 nm)	190 KeV,		
		6 MeV X-rays		
SF_2	Au-NPs	250 KeV X-rays	MDA-MB-231	Velten and Tome (2023)
SF_8	(50 nm)			
SF_2	Au-NPs	Cs-137	A431	Tsai et al. (2022)
SF_4	(50 nm)			
SF_8				
SF_2	AgNPs	6 MeV X-rays	U251	Zhao et al. (2021)
SF_4	(18 nm)			
SF_6				
SF_8				
SF_2	Pt-NPs	Cs-137	MDA-MB-231	Hullo et al. (2021)
SF_4	(20–25 nm)		T47D	
SF_6				

TABLE 2 Overview of Mean Inactivation Dose (MID) used in nanoparticle studies.

Enhancement factor used	NP material (size)	Radiation source	Cell line	Reference
MID	Au-NPs	160 KeV X-rays	MDA-MB-231	Jain et al. (2011)
	(1.9 nm)	6 MeV X-rays	DU145	
		15 MeV X-rays	L132	
	Au-NPs	160 KeV X-rays	MDA-MB-231	Jain et al. (2014)
	(1.9 nm)			
	Au-NPs	6 MeV X-rays	MDA-MB-231	McMahon et al. (2011)
	(2 nm)	15 MeV X-rays		
	Glu-GNPs	6 MeV X-rays	MDA-MB-231	Wang et al. (2015)
	(16 nm or 49 nm)			

oxidation, photobleaching, and interference from intracellular thiols or metal ions often lead to false positives or underestimation (Stergioula et al., 2023). For example, studies involving AuNPs found differences in ROS quantification when comparing H_2DCF-DA with ESR, which has lower sensitivity, requires higher sample-volumes, and cannot resolve spatial-temporal dynamics in biological systems (Stergioula et al., 2023). Similarly, DNA damage quantification relies heavily on γ-H_2AX foci imaging, a marker for DSBs (Figures 3A,B). This method is semi-quantitative and accessible, but cannot distinguish between direct radiation-induced damage and NP-specific chemical interactions, potentially overestimating therapeutic efficacy (Bemidinezhad et al., 2024).

Recent studies show that high-Z NPs enhance both ROS and DNA damage (Figures 3C,D). For example, Au@AgBiS core-shell NPs increased ROS generation by 2.3 times compared to radiation alone, as validated by fluorescent probes and ESR (Xiao et al., 2023). Hafnium-based NPs like $NBTXR_3$ increased DSBs by 40% in melanoma models, quantified by γ-H_2AX foci and comet assays, and correlated with better tumor control in preclinical trials (Zheng and Sanche, 2023). However, inconsistencies arise when linking *in vitro* quantification to clinical outcomes. For example, superparamagnetic iron oxide NPs (SPIONs) showed persistent γ-H_2AX foci in melanoma cells, indicating unrepairable DNA damage, but their clinical translation is limited due to unresolved toxicity and off-target effects (Bemidinezhad et al., 2024).

4.4 Survival and tumor dynamics: from median survival time to growth inhibition

In vivo evaluation of high-Z NP radiosensitization uses various metrics to measure survival benefits and tumor response (Table 4). Median survival time (MST) is a key endpoint, indicating survival benefits and often correlated with tumor control and treatment durability. For example, glioblastoma-bearing mice treated with PEGylated-gold nanoparticles had an MST of 28 days, compared to 14 days in controls, showing the radiosensitizing potential of targeted NPs (Figure 4A) (Yang et al., 2022). mAuNPs alone showed no improvement in survival of B16-F10 cell-bearing mice (16 days, similar to PBS controls), combined therapy with carbon ion irradiation extended survival to 42 days (Figure 4B). In HER3-expressing tumor models, Z-ABD-Z-mcDM1 conjugates extended MST from 68 days for monotherapy to 90 days by enhancing radiation-triggered drug release (Zhang et al., 2024). Similarly, Lu-FAP-2287, a lutetium-based radiopharmaceutical, combined with anti-PD-1 immunotherapy, suppressed tumor growth and extended survival in fibrosarcoma models (Chen et al., 2024). Tumor volume tripling time (TVTT), another metric, reflects regrowth kinetics and provides additional insights. Studies on pancreatic cancer revealed median volume doubling times (VDT) of 40 days, with growth rates inversely correlated to tumor size (Figure 4C) (Hussain et al., 2023). Tumor growth inhibition (TGI), which measures the reduction in tumor volume compared to untreated controls, includes both cytostatic and cytotoxic effects. For example, Gd2O3@BSA-Au NPs achieved 50% TGI in 4T1 tumor-bearing mice, (Figure 4D) (Kim et al., 2024). Notably, NPs like CMP (cationic polymer-coated Au NPs) combined with irreversible electroporation (IRE) achieved over 80% TGI and extended survival in mice by enhancing immunogenic cell death (Atkinson et al., 2025). These metrics connect preclinical findings to clinical relevance, aiding dose optimization and mechanistic validation.

Although MST and TGI are prevalent in current studies, integrating tumor volume kinetics and temporal heterogeneity could enhance outcome predictions. Faster-growing tumors might need higher NP concentrations or fractionated radiation to boost TGI (Feucht et al., 2024). The correlation between NP retention time and MST highlights the importance of pharmacokinetic optimization. However, challenges like standardizing growth rate measurements and dealing with interspecies variability in NP biodistribution remain (Xu et al., 2022). Future research could investigate multimodal imaging with dynamic TGI modeling for personalized NP-enhanced radiotherapy. In summary, *in vivo* quantitative metrics such as MST, TVTT, and TGI are crucial for understanding the therapeutic potential of high-Z NPs. Combining these metrics with mechanistic studies and advanced imaging will speed up the development of precision radiosensitization strategies.

5 Discussion

The quantification of radiosensitization effects mediated by high-Z NPs remains a critical yet contentious topic due to the

TABLE 3 Overview of Dose Enhancement Factor (DEF) and Sensitizer Enhancement Ratio (SER) used in NP studies.

Enhancement factor used	NP material (size)	Radiation source	Cell line	Reference
DEF	Au-NP	225 KeV X-rays	MDA-MB-231	Taggart et al. (2014)
	(1.9 nm)		DU-145	
			T98G	
	Au-NP	160 KeV X-rays	DU-145	Butterworth et al. (2010)
	(1.9 nm)		MDA-231-B	
			MCF-7	
			L-132	
			T98G	
			AGO-1522B	
	$NBTXR_3$-NP	6 MeV X-rays	HT1080 Co-60	Maggiorella et al. (2012)
	(50 nm)			
	Au-NP	6 MeV X-rays	Gel	Behrouzkia et al. (2019)
	(30 nm, 50 nm)			
	Au-NP	6 MeV X-rays	C-33a	Gray et al. (2023)
	(30 nm)	18 MeV X-rays		
	Au-NP	^{192}Ir	Monte Carlo	Gray et al. (2020)
	(30 nm)			
	Au-NP	10 to 370 KeV X-rays	Monte Carlo	Martinov et al. (2023)
SER	Au-NP	6 MeV X-rays	MDA-MB-231	Wang et al. (2015)
	(16 nm)			
	Au-NP	26 KeV X-rays	HCT116	Shi et al. (2016)
	(2.7 nm)			
	Ag-NP	6 MeV X-ray	U251	Liu et al. (2018)
	(27 nm)		C6	
	Alb-Au-NPs	6 MeV X-ray	A549	Chen et al. (2023)
	(205 nm)			
	PSMA-AuNPs	6 MeV X-ray	Monte Carlo	Schmidt et al. (2022)
	Ag@Au NPs	6 MeV X-ray	U87	Li et al. (2022)
	(11 nm)			
	Pt-NPs	Cs-137	HeLa cells	Yang et al. (2020)
	(14.6 nm)			

heterogeneity of experimental models, radiation parameters, and biological endpoints. Metrics like DEF and SER derived from the LQ model offer simplified frameworks for comparing NP efficacy. However, these metrics often overlook the complex interaction between physical dose enhancement and biological mechanisms, such as ROS-mediated DNA damage and immune modulation (Tabatabaie et al., 2022). DEF calculations usually assume uniform NP distribution and ignore localized ROS bursts, which can amplify DNA damage independently of physical dose deposition (Zheng and Sanche, 2023). Similarly, SER values derived from clonogenic survival assays (SF) fail to consider immune-mediated bystander effects, a phenomenon increasingly recognized in NP-aided radiotherapy (Zhang et al., 2023). Furthermore, SF and MID do not account for the tumor microenvironment (TME). ROS quantification relies on error-prone fluorescent probes, while DNA damage assays overlook repair dynamics.

In vivo metrics, such as MST and TGI, struggle to separate NP-specific radiosensitization from off-target immune effects. While Hf-based NPs demonstrate enhanced tumor control via combined dose enhancement and immune activation (Choi et al., 2023), traditional

TABLE 4 Parts of quantifying factors used *in vivo* studies.

Enhancement factor used	NP material (size)	Radiation source	Animal model	Reference
Median survival time	Au-NPs	175 KeV X-rays	U251 orthotopic mouse model	Joh et al. (2013)
	(23 nm)			
	Ag-NPs	6 MeV X-rays	U251 orthotopic mouse model	Liu et al. (2016)
	(27 nm)			
	Ag-NPs	6 MeV X-rays	C6 orthotopic rat model	Liu et al. (2013)
	(88 nm)	(200 MU per minute)		
	IONPs	320 KeV X-rays	U87MG orthotopic mouse model	Bouras et al. (2015)
	(10 nm)	(1.2 Gy per minute)		
	Gd-NPs	90 KeV X-rays	9LGS orthotopic rat model	Le Duc et al. (2014)
	(2.1 nm)			
Tumor volume tripling time	Au-NPs	250 KeV X-rays	U87MG subcutaneous mouse model	Bhattarai et al. (2017)
	(61 nm)			
Tumor growth inhibition	Au-NPs	100 KeV X-rays	MDA-MB-361 subcutaneous mouse model	Chattopadhyay et al. (2013)
	(30 nm)			
	Au-NPs	Cs-137	U14 subcutaneous mouse model	Zhang et al. (2012)
	(4.8, 12.1, 27.3 46.6 nm)			
	Gd_2O_3@BSA-Au NPs	6 MeV X-rays	4T1 subcutaneous mouse model	Nosrati et al. (2023)
	(13 nm)			
	Au-NPs	Carbon Ion Irradiation	B16-F10 subcutaneous mouse model	Zhang et al. (2021)
	(14 nm)			

endpoints like TVTT may mix these mechanisms, leading to overestimations of pure physical sensitization (Zou et al., 2024). Immune-related metrics such as cytokine profiling and T-cell infiltration are rarely integrated into current quantification systems, despite evidence that NPs like Au and Se modulate the TME to synergize with radiotherapy (Forenzo and Larsen, 2024).

Among current metrics, DEF is a crucial metric to compare the radiation amplification potential of different NP compositions and optimize their physicochemical properties, such as size, concentration, and atomic number. For example, studies have demonstrated DEF values ranging from 1.09 to 1.32 for iron oxide NPs and up to 22.17% enhancement for FeO@AuNPs under magnetic field guidance (Fathy et al., 2022). This highlights DEF's utility in quantifying localized energy deposition. The necessity of DEF lies in its ability to connect theoretical predictions with experimental validations, enabling researchers to correlate NP-induced physical dose escalation with biological outcomes, such as tumor cell death (Diaz-Galindo and Garnica-Garza, 2024). However, DEF calculations often oversimplify the complex interplay between physical dose enhancement and biological mechanisms, such as ROS generation, DNA repair inhibition, and immune modulation (Hernandez Millares et al., 2024). Hernández Millares et al. demonstrated that while GNPs achieved a 9-fold DEF under 300 kVp X-rays, biological mechanisms dominated radiosensitization under 6 MV irradiation (DEF ≤10%), evidenced by a lethality enhancement factor (LEF) of 3–4x at low doses. Integrating LEF reduced computational deviations in SER to ≤3.2%, underscoring the necessity of coupling physical and biological effects for accurate modeling.Moreover, DEF measurements are highly sensitive to experimental conditions, including NP distribution heterogeneity within tumors, coating layer composition, and irradiation energy (Gerken et al., 2024). Coating materials, often ignored in DEF-centric studies, can reduce dose enhancement by decreasing NP-tissue interfacial interactions, leading to misleading conclusions about NP performance (Mansouri et al., 2023). DEF's clinical relevance is also debated, as its predictive power diminishes with MeV X-rays due to reduced photoelectric effects, raising questions about its translatability to human radiotherapy (Gerken et al., 2024). Therefore, DEF must be supplemented with auxiliary data to enhance interpretability, such as ROS validation through ESR or CRISPR-based biosensors, immune profiling by quantifying $CD8^+$ T-cell density to assess abscopal effects, and NP biodistribution verification via PET/CT imaging with radiolabeled NPs like ^{64}Cu-AuNPs. In conclusion, while DEF remains a valuable tool for initial screening of NP radiosensitizers, its limitations necessitate a more holistic evaluation framework.

Future research on radiosensitization quantification using high-Z NPs should prioritize standardized radiation energy protocols to isolate NP-specific effects across preclinical (220 KeV) and clinical

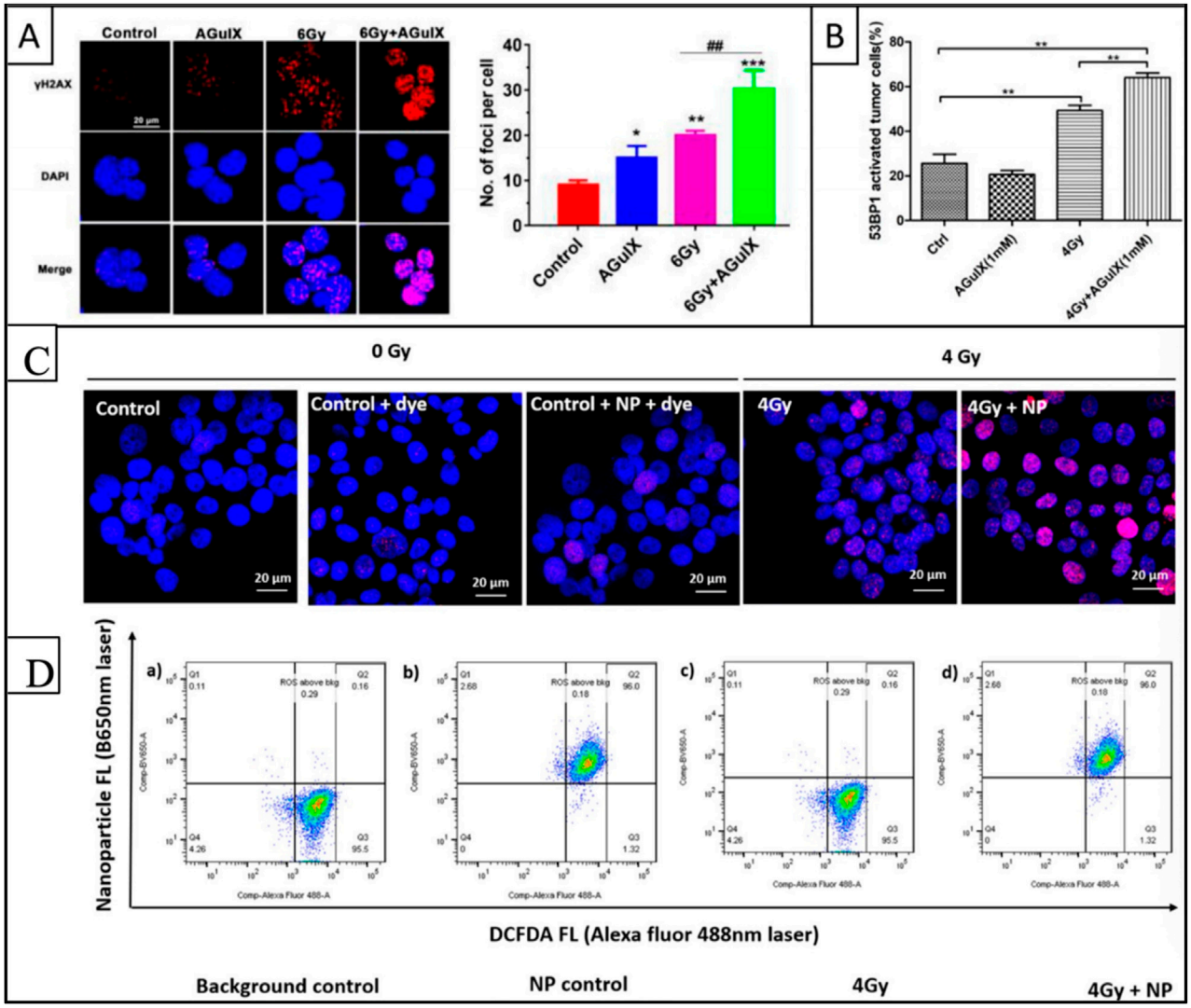

FIGURE 3
Quantification of DNA damage and ROS generation with radiation in the presence of high-Z nanoparticles. **(A)** Fluorescence images representing γ-H2AX foci formation in B16 cells after 6 Gy irradiation and AGuIX incubation (left). Quantification of the γ-H2AX foci in each cell, representing DNA damage (right). **(B)** Quantification of the 53BP1 foci representing DNA strand breaks in H1299 activated cells after 4 Gy irradiation and AGuIX incubation, 24 h post-irradiation. **(C)** Studies in human tongue cancer Cal27 cells using γH2AX to detect DNA damage showed more foci when gold nanoparticles were combined with a single 4-Gy photon dose. **(D)** Flow cytometry quantification of 2′,7′ -Dichlorofluorescin (DCF) revealed elevated ROS levels in gold nanoparticle-treated cells exposed to 4-Gy radiation from a Cesium-137 source. Reproduced with permission of Creative Common Attribution license (Dubey et al., 2022; Aubrun et al., 2025).

(6 MeV) beam energies. Additionally, the radiosensitization efficacy of high-Z NPs is dictated by their material-specific physicochemical properties, such as tunable surface engineering, multimodal imaging compatibility, and high atomic number-driven secondary electron emission. Standardizing synthesis protocols is essential to unify dose enhancement metrics and accelerate clinical translation of these nanoplatforms. A critical advancement lies in multiscale modeling frameworks that integrate Monte Carlo simulations for physical dose deposition, spatiotemporal ROS kinetics, and immune microenvironment dynamics to connect nanoscale energy transfer with macroscale therapeutic outcomes. Furthermore, immune-inclusive endpoints such as abscopal response rates must be included to evaluate systemic antitumor effects mediated by NP-enhanced radiotherapy. The development of a multidimensional Radiosensitization Index (RSI) is proposed as a unifying metric, encompassing: a physical dimension using DEF or SER standardized to clinical (6 MeV) and preclinical (220 KeV) beam energies; a chemical dimension measuring ROS yields through ESR or catalytic activity; a biological dimension tracking γ-H_2AX foci kinetics and circulating tumor DNA (ctDNA) clearance rates; an immunological dimension assessing $CD8^+$/$FoxP3^+$T-cell ratios and PD-L1 expression dynamics; and a clinical dimension based on RECIST-defined TGI and progression-free survival (PFS). This framework integrates physical-chemical interactions, biological damage cascades, immune reprogramming, and clinical translatability, providing a robust platform for cross-disciplinary optimization of NP-enhanced radiotherapy.

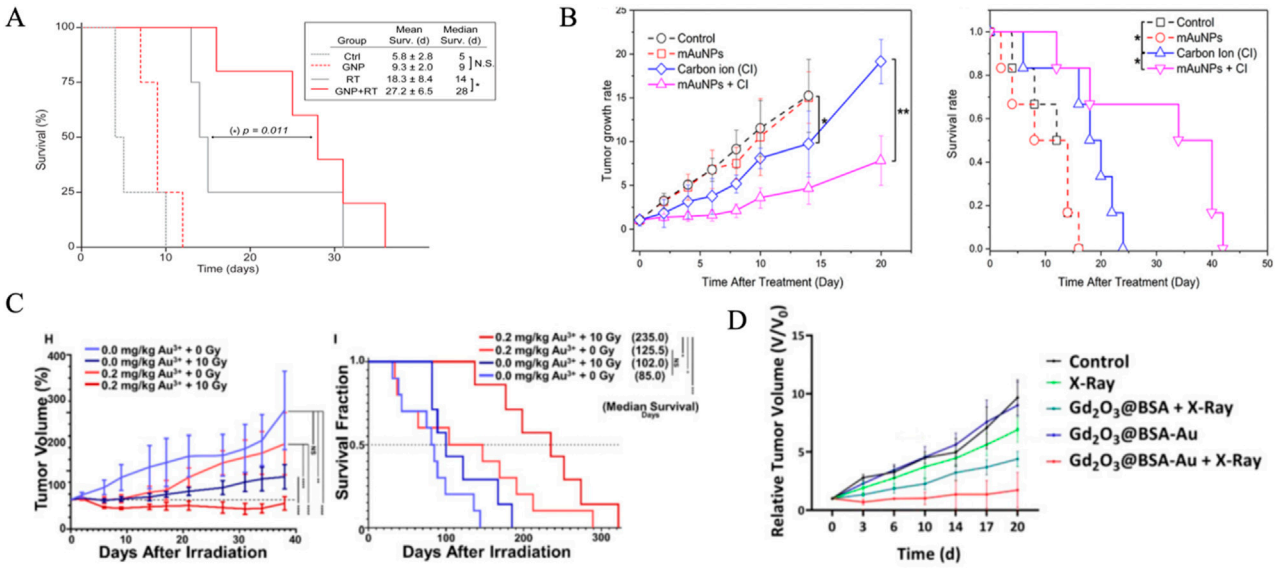

FIGURE 4
In vivo evaluation of high-Z NP radiosensitization effect. **(A)** GNP administration in combination with RT improves survival in mice with advanced GBM tumors.Median and mean survival analysis were obtained with Kaplan–Meier analysis, and comparison between RT *versus* GNP + RT survival curves showed p = 0.011. Mean survival times are shown with 95% confidence intervals. **(B)** Effects of AuNPs on tumor size and survival in mice. (left) Tumor growth rates of the mice in the different groups; (right) Survival of the tumor-bearing mice in the different groups (*, $p < 0.05$; **, $p < 0.01$). **(C)** Normalized tumor volume measurements (H) and survival fractions (I) over time for different treatments with Au3+ (0.0 or 0.2 mg/kg) and radiation (0 or 10 Gy). **(D)** Relative tumor volume of mice treated with various treatment plans. Reproduced with permission of Creative Common Attribution license (Joh et al., 2013; Zhang et al., 2021; Nosrati et al., 2023; Schwartz-Duval et al., 2024).

6 Conclusion

High-Z nanoparticles hold transformative potential for precision radiotherapy by enabling tumor-selective dose amplification through physical, chemical, and biological synergies. However, their clinical translation faces challenges due to fragmented quantification methods, oversimplified models that neglect TME complexity, and inconsistent preclinical-to-clinical correlations. Current metrics do not account for immune modulation, stromal interactions, and nanoparticle heterogeneity, all of which impact therapeutic outcomes. To advance this field, standardizing radiosensitization protocols, using 3D/organoid platforms that mimic TME dynamics, and co-developing multifunctional NPs with diagnostic and therapeutic capabilities are essential. Future success relies on collaboration among radiobiologists, nanotechnologists, and clinicians to validate multidimensional radiosensitization indices in robust trials. Though challenges remain, integrating advanced models, scalable synthesis, and immune-aware design strategies will speed up the clinical adoption of high-Z NPs, improving radiotherapy for resistant cancers.

Author contributions

YL: Writing – original draft, Writing – review and editing, Conceptualization, Funding acquisition, Supervision, Resources, Formal Analysis, Methodology, Investigation.

Funding

The author(s) declare that financial support was received for the research and/or publication of this article. This work was supported by the National Natural Science Foundation of China (No. 82272755), Chongqing Science and Technology Commission (No. 2022NSCQ-MSX0706) and Fundamental Research Funds for the Central Universities (No. 2022CDJYGRH-007).

Acknowledgments

The author thanks YN.Y., Q.L. CB.F., and QS. L. for their informal feedback during the preparation of this work.

Conflict of interest

The author declares that the research was conducted in the absence of any commercial or financial relationships that could be construed as a potential conflict of interest.

Generative AI statement

The author(s) declare that no Generative AI was used in the creation of this manuscript.

Publisher's note

References

Abdollahi, H., Yousefirizi, F., Shiri, I., Brosch-Lenz, J., Mollaheydar, E., Fele-Paranj, A., et al. (2024). Theranostic digital twins: concept, framework and roadmap towards personalized radiopharmaceutical therapies. *Theranostics* 14 (9), 3404–3422. doi:10.7150/thno.93973

Alex, J., and Mathew, T. V. (2023). Surface modification of Bi(2)O(3) nanoparticles with biotinylated beta-cyclodextrin as a biocompatible therapeutic agent for anticancer and antimicrobial applications. *Molecules* 28 (8), 3604. doi:10.3390/molecules28083604

Alkotub, B., Bauer, L., Bashiri Dezfouli, A., Hachani, K., Ntziachristos, V., Multhoff, G., et al. (2025). Radiosensitizing capacity of fenofibrate in glioblastoma cells depends on lipid metabolism. *Redox Biol.* 79, 103452. doi:10.1016/j.redox.2024.103452

Atkinson, J., Chopin, J., Bezak, E., Le, H., and Kempson, I. (2025). Gold nanoparticles cause radiosensitization in 4T1 cells by inhibiting DNA double strand break repair: single cell comparisons of DSB formation and γH2AX expression. *Chemphyschem* 26 (3), e202400764. doi:10.1002/cphc.202400764

Aubrun, C., Doussineau, T., Carmes, L., Meyzaud, A., Boux, F., Dufort, S., et al. (2025). Mechanisms of action of AGuIX as a pan-cancer nano-radiosensitizer: a comprehensive review. *Pharm. (Basel)* 18 (4), 519. doi:10.3390/ph18040519

Babaye Abdollahi, B., Malekzadeh, R., Pournaghi Azar, F., Salehnia, F., Naseri, A. R., Ghorbani, M., et al. (2021). Main approaches to enhance radiosensitization in cancer cells by nanoparticles: a systematic review. *Adv. Pharm. Bull.* 11 (2), 212–223. doi:10.34172/apb.2021.025

Bai, L., Jiang, F., Wang, R., Lee, C., Wang, H., Zhang, W., et al. (2020). Ultrathin gold nanowires to enhance radiation therapy. *J. Nanobiotechnology* 18 (1), 131. doi:10.1186/s12951-020-00678-3

Balke, J., Volz, P., Neumann, F., Brodwolf, R., Wolf, A., Pischon, H., et al. (2018). Visualizing oxidative cellular stress induced by nanoparticles in the subcytotoxic range using fluorescence lifetime imaging. *Small* 14 (23), e1800310. doi:10.1002/smll.201800310

Baumann, M., Krause, M., Overgaard, J., Debus, J., Bentzen, S. M., Daartz, J., et al. (2016). Radiation oncology in the era of precision medicine. *Nat. Rev. Cancer* 16 (4), 234–249. doi:10.1038/nrc.2016.18

Behrouzkia, Z., Zohdiaghdam, R., Khalkhali, H. R., and Mousavi, F. (2019). Evaluation of gold nanoparticle size effect on dose enhancement factor in megavoltage beam radiotherapy using MAGICA polymer gel dosimeter. *J. Biomed. Phys. Eng.* 9 (1), 89–96. doi:10.31661/jbpe.v0i0.1019

Bemidinezhad, A., Radmehr, S., Moosaei, N., Efati, Z., Kesharwani, P., and Sahebkar, A. (2024). Enhancing radiotherapy for melanoma: the promise of high-Z metal nanoparticles in radiosensitization. *Nanomedicine (Lond).* 19 (28), 2391–2411. doi:10.1080/17435889.2024.2403325

Bhattarai, S. R., Derry, P. J., Aziz, K., Singh, P. K., Khoo, A. M., Chadha, A. S., et al. (2017). Gold nanotriangles: scale up and X-ray radiosensitization effects in mice. *Nanoscale* 9 (16), 5085–5093. doi:10.1039/c6nr08172j

Bouras, A., Kaluzova, M., and Hadjipanayis, C. G. (2015). Radiosensitivity enhancement of radioresistant glioblastoma by epidermal growth factor receptor antibody-conjugated iron-oxide nanoparticles. *J. Neurooncol* 124 (1), 13–22. doi:10.1007/s11060-015-1807-0

Bray, F., Laversanne, M., Sung, H., Ferlay, J., Siegel, R. L., Soerjomataram, I., et al. (2024). Global cancer statistics 2022: GLOBOCAN estimates of incidence and mortality worldwide for 36 cancers in 185 countries. *CA Cancer J. Clin.* 74 (3), 229–263. doi:10.3322/caac.21834

Busato, F., Khouzai, B. E., and Mognato, M. (2022). Biological mechanisms to reduce radioresistance and increase the efficacy of radiotherapy: state of the art. *Int. J. Mol. Sci.* 23 (18), 10211. doi:10.3390/ijms231810211

Butterworth, K. T., Coulter, J. A., Jain, S., Forker, J., Mcmahon, S. J., Schettino, G., et al. (2010). Evaluation of cytotoxicity and radiation enhancement using 1.9 nm gold particles: potential application for cancer therapy. *Nanotechnology* 21 (29), 295101. doi:10.1088/0957-4484/21/29/295101

Cai, C., Liu, Y., Zhang, Z., Tian, T., Wang, Y., Wang, L., et al. (2023). Activity-based self-enriched SERS sensor for blood metabolite monitoring. *ACS Appl. Mater Interfaces* 15 (4), 4895–4902. doi:10.1021/acsami.2c18261

Chattopadhyay, N., Cai, Z., Kwon, Y. L., Lechtman, E., Pignol, J. P., and Reilly, R. M. (2013). Molecularly targeted gold nanoparticles enhance the radiation response of breast cancer cells and tumor xenografts to X-radiation. *Breast Cancer Res. Treat.* 137 (1), 81–91. doi:10.1007/s10549-012-2338-4

Chen, H. Y., He, Y., Wang, X. Y., Ye, M. J., Chen, C., Qian, R. C., et al. (2025). Deep learning-assisted surface-enhanced Raman spectroscopy detection of intracellular reactive oxygen species. *Talanta* 284, 127222. doi:10.1016/j.talanta.2024.127222

Chen, L. C., Lin, H. Y., Hung, S. K., Chiou, W. Y., and Lee, M. S. (2021). Role of modern radiotherapy in managing patients with hepatocellular carcinoma. *World J. Gastroenterol.* 27 (20), 2434–2457. doi:10.3748/wjg.v27.i20.2434

Chen, J., Qu, X., Qi, G., Xu, W., Jin, Y., and Xu, S. (2022). Electrostimulus-triggered reactive oxygen species level in organelles revealed by organelle-targeting SERS nanoprobes. *Anal. Bioanal. Chem.* 414 (23), 6965–6975. doi:10.1007/s00216-022-04265-3

Chen, X., Song, J., Chen, X., and Yang, H. (2019). X-ray-activated nanosystems for theranostic applications. *Chem. Soc. Rev.* 48 (11), 3073–3101. doi:10.1039/c8cs00921j

Chen, Y., Liu, S., Liao, Y., Yang, H., Chen, Z., Hu, Y., et al. (2023). Albumin-modified gold nanoparticles as novel radiosensitizers for enhancing lung cancer radiotherapy. *Int. J. Nanomedicine* 18, 1949–1964. doi:10.2147/IJN.S398254

Chen, Y., Yang, J., Fu, S., and Wu, J. (2020). Gold nanoparticles as radiosensitizers in cancer radiotherapy. *Int. J. Nanomedicine* 15, 9407–9430. doi:10.2147/IJN.S272902

Chen, Z., Long, L., Wang, J., Jiang, M., Li, W., Cui, W., et al. (2024). Enhanced tumor site accumulation and therapeutic efficacy of extracellular matrix-drug conjugates targeting tumor cells. *Small* 20 (40), e2402040. doi:10.1002/smll.202402040

Choi, B. J., Jung, K. O., Graves, E. E., and Pratx, G. (2018). A gold nanoparticle system for the enhancement of radiotherapy and simultaneous monitoring of reactive-oxygen-species formation. *Nanotechnology* 29 (50), 504001. doi:10.1088/1361-6528/aae272

Choi, E., Landry, M., Pennock, N., Neufeld, M., Weinfurter, K., Goforth, A., et al. (2023). Nanoscale hafnium metal-organic frameworks enhance radiotherapeutic effects by upregulation of type I interferon and TLR7 expression. *Adv. Healthc. Mater* 12 (13), e2202830. doi:10.1002/adhm.202202830

Chow, J. C. L., and Jubran, S. (2023). Depth dose enhancement in orthovoltage nanoparticle-enhanced radiotherapy: a Monte Carlo phantom study. *Micromachines (Basel).* 14 (6), 1230. doi:10.3390/mi14061230

Chun, S. G., Hu, C., Komaki, R. U., Timmerman, R. D., Schild, S. E., Bogart, J. A., et al. (2024). Long-term prospective outcomes of intensity modulated radiotherapy for locally advanced lung cancer: a secondary analysis of a randomized clinical trial. *JAMA Oncol.* 10 (8), 1111–1115. doi:10.1001/jamaoncol.2024.1841

Coulter, J. A., Jain, S., Butterworth, K. T., Taggart, L. E., Dickson, G. R., Mcmahon, S. J., et al. (2012). Cell type-dependent uptake, localization, and cytotoxicity of 1.9 nm gold nanoparticles. *Int. J. Nanomedicine* 7, 2673–2685. doi:10.2147/IJN.S31751

Cui, L., Tse, K., Zahedi, P., Harding, S. M., Zafarana, G., Jaffray, D. A., et al. (2014). Hypoxia and cellular localization influence the radiosensitizing effect of gold nanoparticles (AuNPs) in breast cancer cells. *Radiat. Res.* 182 (5), 475–488. doi:10.1667/RR13642.1

Das, B. (2025). Transition metal complex-loaded nanosystems: advances in stimuli-responsive cancer therapies. *Small* 21 (7), e2410338. doi:10.1002/smll.202410338

Deng, H., Chen, Y., Li, P., Hang, Q., Zhang, P., Jin, Y., et al. (2023). PI3K/AKT/mTOR pathway, hypoxia, and glucose metabolism: potential targets to overcome radioresistance in small cell lung cancer. *Cancer Pathog. Ther.* 1 (1), 56–66. doi:10.1016/j.cpt.2022.09.001

Diaz-Galindo, C. A., and Garnica-Garza, H. M. (2024). Gold nanoparticle-enhanced radiotherapy: dependence of the macroscopic dose enhancement on the microscopic localization of the nanoparticles within the tumor vasculature. *PLoS One* 19 (7), e0304670. doi:10.1371/journal.pone.0304670

Ding, X., Liang, S., Zhang, T., Zhang, M., Fang, H., Tian, J., et al. (2025a). Surface modification of gold nanoparticle impacts distinct lipid metabolism. *Molecules* 30 (8), 1727. doi:10.3390/molecules30081727

Ding, X., Lu, Q., Liu, J., Fu, Q., Jiang, L., and Huang, Y. (2025b). Precise fabrication of spatially engineered brochosomes for *in-situ* investigation of cellular ROS secretion. *Talanta.* 294, 128245. doi:10.1016/j.talanta.2025.128245

Dubey, P., Sertorio, M., and Takiar, V. (2022). Therapeutic advancements in metal and metal oxide nanoparticle-based radiosensitization for head and neck cancer therapy. *Cancers (Basel)* 14 (3), 514. doi:10.3390/cancers14030514

Fan, H., Wang, L., Zeng, X., Xiong, C., Yu, D., Zhang, X., et al. (2025). Redox-inducible radiomimetic photosensitizers selectively suppress cancer cell proliferation by damaging DNA through radical cation chemistry. *Angew. Chem. Int. Ed. Engl.* 64 (1), e202413352. doi:10.1002/anie.202413352

Fathy, M. M., Saad, O. A., Elshemey, W. M., and Fahmy, H. M. (2022). Dose-enhancement of MCF 7 cell line radiotherapy using silica-iron oxide nanocomposite. *Biochem. Biophys. Res. Commun.* 632, 100–106. doi:10.1016/j.bbrc.2022.09.087

Feucht, D., Haas, P., Skardelly, M., Behling, F., Rieger, D., Bombach, P., et al. (2024). Preoperative growth dynamics of untreated glioblastoma: description of an exponential growth type, correlating factors, and association with postoperative survival. *Neurooncol Adv.* 6 (1), vdae053. doi:10.1093/noajnl/vdae053

Forenzo, C., and Larsen, J. (2024). Bridging clinical radiotherapy and space radiation therapeutics through reactive oxygen species (ROS)-triggered delivery. *Free Radic. Biol. Med.* 219, 88–103. doi:10.1016/j.freeradbiomed.2024.04.219

Franzone, P., Fiorentino, A., Barra, S., Cante, D., Masini, L., Cazzulo, E., et al. (2016). Image-guided radiation therapy (IGRT): practical recommendations of Italian Association of Radiation Oncology (AIRO). *Radiol. Med.* 121 (12), 958–965. doi:10.1007/s11547-016-0674-x

Fu, H., Xie, Y., Ren, S., Zhang, Q., Cheng, J., Liang, Q., et al. (2025). Multifunctional Cu(3)BiS(3)-BP@PEI radiosensitizer with enhanced reactive oxygen species activity for multimodal synergistic therapy. *ACS Biomater. Sci. Eng.* 11 (2), 930–941. doi:10.1021/acsbiomaterials.4c01907

Galloway, T. J., Indelicato, D. J., Amdur, R. J., Morris, C. G., Swanson, E. L., and Marcus, R. B. (2012). Analysis of dose at the site of second tumor formation after radiotherapy to the central nervous system. *Int. J. Radiat. Oncol. Biol. Phys.* 82 (1), 90–94. doi:10.1016/j.ijrobp.2010.10.062

Gerken, L. R. H., Beckers, C., Brugger, B. A., Kissling, V. M., Gogos, A., Wee, S., et al. (2024). Catalytically active Ti-based nanomaterials for hydroxyl radical mediated clinical X-ray enhancement. *Adv. Sci. (Weinh)* 11 (47), e2406198. doi:10.1002/advs.202406198

Gerken, L. R. H., Gerdes, M. E., Pruschy, M., and Herrmann, I. K. (2023). Prospects of nanoparticle-based radioenhancement for radiotherapy. *Mater Horiz.* 10 (10), 4059–4082. doi:10.1039/d3mh00265a

Gimeno-Ferrero, R., De Jesus, J. R., and Leal, M. P. (2024). Efficient strategy to synthesize tunable pH-responsive hybrid micelles based on iron oxide and gold nanoparticles. *Langmuir* 40 (22), 11775–11784. doi:10.1021/acs.langmuir.4c01318

Gray, T. M., David, S., Bassiri, N., Patel, D. Y., Kirby, N., and Mayer, K. M. (2023). Microdosimetric and radiobiological effects of gold nanoparticles at therapeutic radiation energies. *Int. J. Radiat. Biol.* 99 (2), 308–317. doi:10.1080/09553002.2022.2087931

Gray, T., Bassiri, N., David, S., Patel, D. Y., Stathakis, S., Kirby, N., et al. (2020). A detailed Monte Carlo evaluation of (192)Ir dose enhancement for gold nanoparticles and comparison with experimentally measured dose enhancements. *Phys. Med. Biol.* 65 (13), 135007. doi:10.1088/1361-6560/ab9502

Guerra, D. B., Oliveira, E. M. N., Sonntag, A. R., Sbaraine, P., Fay, A. P., Morrone, F. B., et al. (2022). Intercomparison of radiosensitization induced by gold and iron oxide nanoparticles in human glioblastoma cells irradiated by 6 MV photons. *Sci. Rep.* 12 (1), 9602. doi:10.1038/s41598-022-13368-x

Guganathan, L., Rajeevgandhi, C., Sathiyamurthy, K., Thirupathi, K., Santhamoorthy, M., Chinnasamy, E., et al. (2022). Magnetic application of gadolinium orthoferrite nanoparticles synthesized by sol-gel auto-combustion method. *Gels* 8 (11), 688. doi:10.3390/gels8110688

Guruswamy Pandian, A. P., Ramachandran, A. K., Kodaganallur Pitchumani, P., Mathai, B., and Thomas, D. C. (2025). Evaluation of anti-biofilm property of zirconium oxide nanoparticles on Streptococcus mutans and *Enterococcus faecalis*: an *in vitro* study. *Cureus* 17 (1), e77199. doi:10.7759/cureus.77199

Hernandez Millares, R., Bae, C., Kim, S. J., Kim, T., Park, S. Y., Lee, K., et al. (2024). Clonogenic assay and computational modeling using real cell images to study physical enhancement and cellular sensitization induced by metal nanoparticles under MV and kV X-ray irradiation. *Nanoscale* 16 (14), 7110–7122. doi:10.1039/d3nr06257k

Her, S., Jaffray, D. A., and Allen, C. (2017). Gold nanoparticles for applications in cancer radiotherapy: mechanisms and recent advancements. *Adv. Drug Deliv. Rev.* 109, 84–101. doi:10.1016/j.addr.2015.12.012

Hong, J., Bae, S., Cavinato, L., Seifert, R., Ryhiner, M., Rominger, A., et al. (2024). Deciphering the effects of radiopharmaceutical therapy in the tumor microenvironment of prostate cancer: an in-silico exploration with spatial transcriptomics. *Theranostics* 14 (18), 7122–7139. doi:10.7150/thno.99516

Huff, C. (2007). Catching the proton wave. *Hosp. Health Netw.* 81 (3), 62, 64, 66, 2–2.

Hullo, M., Grall, R., Perrot, Y., Mathe, C., Menard, V., Yang, X., et al. (2021). Radiation enhancer effect of platinum nanoparticles in breast cancer cell lines: *in vitro* and *in silico* analyses. *Int. J. Mol. Sci.* 22 (9), 4436. doi:10.3390/ijms22094436

Hussain, S., Haider, S., Maqsood, S., Damasevicius, R., Maskeliunas, R., and Khan, M. (2023). ETISTP: an enhanced model for brain tumor identification and survival time prediction. *Diagn. (Basel)* 13 (8), 1456. doi:10.3390/diagnostics13081456

Jain, S., Coulter, J. A., Butterworth, K. T., Hounsell, A. R., Mcmahon, S. J., Hyland, W. B., et al. (2014). Gold nanoparticle cellular uptake, toxicity and radiosensitisation in hypoxic conditions. *Radiother. Oncol.* 110 (2), 342–347. doi:10.1016/j.radonc.2013.12.013

Jain, S., Coulter, J. A., Hounsell, A. R., Butterworth, K. T., Mcmahon, S. J., Hyland, W. B., et al. (2011). Cell-specific radiosensitization by gold nanoparticles at megavoltage radiation energies. *Int. J. Radiat. Oncol. Biol. Phys.* 79 (2), 531–539. doi:10.1016/j.ijrobp.2010.08.044

Jeon, J. K., Han, S. M., Min, S. K., Seo, S. J., Ihm, K., Chang, W. S., et al. (2016). Coulomb nanoradiator-mediated, site-specific thrombolytic proton treatment with a traversing pristine Bragg peak. *Sci. Rep.* 6, 37848. doi:10.1038/srep37848

Joh, D. Y., Sun, L., Stangl, M., Al Zaki, A., Murty, S., Santoiemma, P. P., et al. (2013). Selective targeting of brain tumors with gold nanoparticle-induced radiosensitization. *PLoS One* 8 (4), e62425. doi:10.1371/journal.pone.0062425

Kaercher, B. P., and Lear, B. J. (2025). Using post synthetic treatment of AuNPs to improve uniformity of their thiol ligand coverage and electronic properties. *Inorg. Chem.* 64 (10), 5132–5139. doi:10.1021/acs.inorgchem.4c05446

Kao, W. Y., Yu, S. H., Mai, F. D., and Liu, Y. C. (2025). Plasmon-activated water innovatively applicable for improving the performance of surface-enhanced Raman scattering. *Talanta* 295, 128232. doi:10.1016/j.talanta.2025.128232

Karapiperis, C., Chasapi, A., Angelis, L., Scouras, Z. G., Mastroberardino, P. G., Tapio, S., et al. (2021). The coming of age for big data in systems radiobiology, an engineering perspective. *Big Data* 9 (1), 63–71. doi:10.1089/big.2019.0144

Katrivas, L., Ben-Menachem, A., Gupta, S., and Kotlyar, A. B. (2023). Ultrasmall ATP-coated gold nanoparticles specifically bind to non-hybridized regions in DNA. *Nanomater. (Basel)* 13 (24), 3080. doi:10.3390/nano13243080

Kazmi, F., Vallis, K. A., Vellayappan, B. A., Bandla, A., Yukun, D., and Carlisle, R. (2020). Megavoltage radiosensitization of gold nanoparticles on a glioblastoma cancer cell line using a clinical platform. *Int. J. Mol. Sci.* 21 (2), 429. doi:10.3390/ijms21020429

Khandal, J., Dohare, S., Dongsar, T. S., Gupta, G., Alsayari, A., Wahab, S., et al. (2025). Gelatin nanocarriers in oncology: a biocompatible strategy for targeted drug delivery. *Int. J. Biol. Macromol.* 310 (Pt 1), 143244. doi:10.1016/j.ijbiomac.2025.143244

Kim, T., Millares, R. H., Kim, T., Eom, M., Kim, J., and Ye, S. J. (2024). Nanoscale dosimetry for a radioisotope-labeled metal nanoparticle using MCNP6.2 and Geant4. *Med. Phys.* 51 (12), 9290–9302. doi:10.1002/mp.17371

Kreipl, M. S., Friedland, W., and Paretzke, H. G. (2009). Time- and space-resolved Monte Carlo study of water radiolysis for photon, electron and ion irradiation. *Radiat. Environ. Biophys.* 48 (1), 11–20. doi:10.1007/s00411-008-0194-8

Kunoh, T., Shimura, T., Kasai, T., Matsumoto, S., Mahmud, H., Khayrani, A. C., et al. (2019). Use of DNA-generated gold nanoparticles to radiosensitize and eradicate radioresistant glioma stem cells. *Nanotechnology* 30 (5), 055101. doi:10.1088/1361-6528/aaedd5

Le Duc, G., Roux, S., Paruta-Tuarez, A., Dufort, S., Brauer, E., Marais, A., et al. (2014). Advantages of gadolinium based ultrasmall nanoparticles vs molecular gadolinium chelates for radiotherapy guided by MRI for glioma treatment. *Cancer Nanotechnol.* 5 (1), 4. doi:10.1186/s12645-014-0004-8

Lee, C., Liu, X., Zhang, W., Duncan, M. A., Jiang, F., Kim, C., et al. (2021). Ultrasmall Gd@Cdots as a radiosensitizing agent for non-small cell lung cancer. *Nanoscale* 13 (20), 9252–9263. doi:10.1039/d0nr08166c

Li, C., Fang, X., Zeng, Q., Zeng, L., Zhang, B., and Nie, G. (2024). Ultra small gold nanoclusters supported on two-dimensional bismuth selenium nanosheets for synergistic photothermal and photodynamic tumor therapy. *RSC Adv.* 14 (33), 24335–24344. doi:10.1039/d4ra03142c

Li, D., Zhao, J., Ma, J., Yang, H., Zhang, X., Cao, Y., et al. (2022). GMT8 aptamer conjugated PEGylated Ag@Au core-shell nanoparticles as a novel radiosensitizer for targeted radiotherapy of glioma. *Colloids Surf. B Biointerfaces* 211, 112330. doi:10.1016/j.colsurfb.2022.112330

Liu, D., Wang, H., Yang, W., Bai, Y., Wu, Z., Cui, T., et al. (2025). One-dose bioorthogonal gadolinium nanoprobes for prolonged radiosensitization of tumor. *Small* 21, e2500504. doi:10.1002/smll.202500504

Liu, J., Wu, J., Chen, T., Yang, B., Liu, X., XI, J., et al. (2024). Enhancing X-ray sensitization with multifunctional nanoparticles. *Small* 20 (35), e2400954. doi:10.1002/smll.202400954

Liu, P., Huang, Z., Chen, Z., Xu, R., Wu, H., Zang, F., et al. (2013). Silver nanoparticles: a novel radiation sensitizer for glioma? *Nanoscale* 5 (23), 11829–11836. doi:10.1039/c3nr01351k

Liu, P., Jin, H., Guo, Z., Ma, J., Zhao, J., Li, D., et al. (2016). Silver nanoparticles outperform gold nanoparticles in radiosensitizing U251 cells *in vitro* and in an intracranial mouse model of glioma. *Int. J. Nanomedicine* 11, 5003–5014. doi:10.2147/IJN.S115473

Liu, Z., Tan, H., Zhang, X., Chen, F., Zhou, Z., Hu, X., et al. (2018). Enhancement of radiotherapy efficacy by silver nanoparticles in hypoxic glioma cells. *Artif. Cells Nanomed Biotechnol.* 46 (Suppl. 3), S922–S930. doi:10.1080/21691401.2018.1518912

Maggiorella, L., Barouch, G., Devaux, C., Pottier, A., Deutsch, E., Bourhis, J., et al. (2012). Nanoscale radiotherapy with hafnium oxide nanoparticles. *Future Oncol.* 8 (9), 1167–1181. doi:10.2217/fon.12.96

Mancuso, M., Pasquali, E., Giardullo, P., Leonardi, S., Tanori, M., Di Majo, V., et al. (2012). The radiation bystander effect and its potential implications for human health. *Curr. Mol. Med.* 12 (5), 613–624. doi:10.2174/156652412800620011

Mansouri, E., Mesbahi, A., Hamishehkar, H., Montazersaheb, S., Hosseini, V., and Rajabpour, S. (2023). The effect of nanoparticle coating on biological, chemical and

biophysical parameters influencing radiosensitization in nanoparticle-aided radiation therapy. *BMC Chem.* 17 (1), 180. doi:10.1186/s13065-023-01099-7

Mansouri, E., Rajabpour, S., and Mesbahi, A. (2024). *In silico* estimation of polyethylene glycol coating effect on metallic NPs radio-sensitization in kilovoltage energy beams. *BMC Chem.* 18 (1), 206. doi:10.1186/s13065-024-01322-z

Martinez-Rovira, I., and Prezado, Y. (2015). Evaluation of the local dose enhancement in the combination of proton therapy and nanoparticles. *Med. Phys.* 42 (11), 6703–6710. doi:10.1118/1.4934370

Martinov, M. P., Fletcher, E. M., and Thomson, R. M. (2023). Multiscale Monte Carlo simulations of gold nanoparticle dose-enhanced radiotherapy I: cellular dose enhancement in microscopic models. *Med. Phys.* 50 (9), 5853–5864. doi:10.1002/mp.16454

Mckinnon, S., Guatelli, S., Incerti, S., Ivanchenko, V., Konstantinov, K., Corde, S., et al. (2016). Local dose enhancement of proton therapy by ceramic oxide nanoparticles investigated with Geant4 simulations. *Phys. Med.* 32 (12), 1584–1593. doi:10.1016/j.ejmp.2016.11.112

Mcmahon, S. J., Hyland, W. B., Muir, M. F., Coulter, J. A., Jain, S., Butterworth, K. T., et al. (2011). Nanodosimetric effects of gold nanoparticles in megavoltage radiation therapy. *Radiother. Oncol.* 100 (3), 412–416. doi:10.1016/j.radonc.2011.08.026

Meng, T. Z., Yang, L. I., Xiang, JINGFENG, Zhu, DAOMING, Ligang, X. I. A., Bin, G. U. O., et al. (2023). AIEgen-based nanotherapeutic strategy for enhanced FLASH irradiation to prevent tumour recurrence and avoid severe side effects. *Chem. Eng. J.* 473, 145179. doi:10.1016/j.cej.2023.145179

Mesbahi, A., Rajabpour, S., Smilowitz, H. M., and Hainfeld, J. F. (2022). Accelerated brachytherapy with the Xoft electronic source used in association with iodine, gold, bismuth, gadolinium, and hafnium nano-radioenhancers. *Brachytherapy* 21 (6), 968–978. doi:10.1016/j.brachy.2022.06.008

Mirjolet, C., Papa, A. L., Crehange, G., Raguin, O., Seignez, C., Paul, C., et al. (2013). The radiosensitization effect of titanate nanotubes as a new tool in radiation therapy for glioblastoma: a proof-of-concept. *Radiother. Oncol.* 108 (1), 136–142. doi:10.1016/j.radonc.2013.04.004

Moloudi, K., Khani, A., Najafi, M., Azmoonfar, R., Azizi, M., Nekounam, H., et al. (2023). Critical parameters to translate gold nanoparticles as radiosensitizing agents into the clinic. *Wiley Interdiscip. Rev. Nanomed Nanobiotechnol* 15 (6), e1886. doi:10.1002/wnan.1886

Morris, B. B., Heeke, S., XI, Y., Diao, L., Wang, Q., Rocha, P., et al. (2025). DNA damage response signatures are associated with frontline chemotherapy response and routes of tumor evolution in extensive stage small cell lung cancer. *Mol. Cancer* 24 (1), 90. doi:10.1186/s12943-025-02291-0

Morrison, R. A., Rybak-Smith, M. J., Thompson, J. M., Thiebaut, B., Hill, M. A., and Townley, H. E. (2017). Efficacy of radiosensitizing doped titania nanoparticles under hypoxia and preparation of an embolic microparticle. *Int. J. Nanomedicine* 12, 3851–3863. doi:10.2147/IJN.S127341

Mowat, P., Mignot, A., Rima, W., Lux, F., Tillement, O., Roulin, C., et al. (2011). *In vitro* radiosensitizing effects of ultrasmall gadolinium based particles on tumour cells. *J. Nanosci. Nanotechnol.* 11 (9), 7833–7839. doi:10.1166/jnn.2011.4725

Nosrati, H., Salehiabar, M., Charmi, J., Yaray, K., Ghaffarlou, M., Balcioglu, E., et al. (2023). Enhanced *in vivo* radiotherapy of breast cancer using gadolinium oxide and gold hybrid nanoparticles. *ACS Appl. Bio Mater* 6 (2), 784–792. doi:10.1021/acsabm.2c00965

Paganetti, H., Beltran, C., Both, S., Dong, L., Flanz, J., Furutani, K., et al. (2021). Roadmap: proton therapy physics and biology. *Phys. Med. Biol.* 66 (5), 05RM01. doi:10.1088/1361-6560/abcd16

Pan, H., Zhou, L., Cheng, Z., Zhang, J., Shen, N., Ma, H., et al. (2024). Perioperative Tislelizumab plus intensity modulated radiotherapy in resectable hepatocellular carcinoma with macrovascular invasion: a phase II trial. *Nat. Commun.* 15 (1), 9350. doi:10.1038/s41467-024-53704-5

Perry, J., Minaei, E., Engels, E., Ashford, B. G., Mcalary, L., Clark, J. R., et al. (2020). Thulium oxide nanoparticles as radioenhancers for the treatment of metastatic cutaneous squamous cell carcinoma. *Phys. Med. Biol.* 65 (21), 215018. doi:10.1088/1361-6560/abaa5d

Pfeiffer, D., Pfeiffer, F., and Rummeny, E. (2020). Advanced X-ray imaging Technology. *Recent Results Cancer Res.* 216, 3–30. doi:10.1007/978-3-030-42618-7_1

Pi, F., Deng, X., Xue, Q., Zheng, L., Liu, H., Yang, F., et al. (2023). Alleviating the hypoxic tumor microenvironment with MnO(2)-coated CeO(2) nanoplatform for magnetic resonance imaging guided radiotherapy. *J. Nanobiotechnology* 21 (1), 90. doi:10.1186/s12951-023-01850-1

Rahman, W. N., Corde, S., Yagi, N., Abdul Aziz, S. A., Annabell, N., and Geso, M. (2014). Optimal energy for cell radiosensitivity enhancement by gold nanoparticles using synchrotron-based monoenergetic photon beams. *Int. J. Nanomedicine* 9, 2459–2467. doi:10.2147/IJN.S59471

Rajesh, S., Zhai, J., Drummond, C. J., and Tran, N. (2022). Novel pH-responsive cubosome and hexosome lipid nanocarriers of SN-38 are prospective for cancer therapy. *Pharmaceutics* 14 (10), 2175. doi:10.3390/pharmaceutics14102175

Reda, M., Bagley, A. F., Zaidan, H. Y., and Yantasee, W. (2020). Augmenting the therapeutic window of radiotherapy: a perspective on molecularly targeted therapies and nanomaterials. *Radiother. Oncol.* 150, 225–235. doi:10.1016/j.radonc.2020.06.041

Schaue, D., and Mcbride, W. H. (2015). Opportunities and challenges of radiotherapy for treating cancer. *Nat. Rev. Clin. Oncol.* 12 (9), 527–540. doi:10.1038/nrclinonc.2015.120

Schmidt, R. M., Hara, D., Vega, J. D., Abuhaija, M. B., Tao, W., Dogan, N., et al. (2022). Quantifying radiosensitization of PSMA-targeted gold nanoparticles on prostate cancer cells at megavoltage radiation energies by Monte Carlo simulation and local effect model. *Pharmaceutics* 14 (10), 2205. doi:10.3390/pharmaceutics14102205

Schuemann, J., Bagley, A. F., Berbeco, R., Bromma, K., Butterworth, K. T., Byrne, H. L., et al. (2020). Roadmap for metal nanoparticles in radiation therapy: current status, translational challenges, and future directions. *Phys. Med. Biol.* 65 (21), 21RM02. doi:10.1088/1361-6560/ab9159

Schuemann, J., Berbeco, R., Chithrani, D. B., Cho, S. H., Kumar, R., Mcmahon, S. J., et al. (2016). Roadmap to clinical use of gold nanoparticles for radiation sensitization. *Int. J. Radiat. Oncol. Biol. Phys.* 94 (1), 189–205. doi:10.1016/j.ijrobp.2015.09.032

Schwartz-Duval, A. S., Mackeyev, Y., Mahmud, I., Lorenzi, P. L., Gagea, M., Krishnan, S., et al. (2024). Intratumoral biosynthesis of gold nanoclusters by pancreatic cancer to overcome delivery barriers to radiosensitization. *ACS Nano* 18 (3), 1865–1881. doi:10.1021/acsnano.3c04260

Shen, H., Wang, H., Mo, J., Zhang, J., Xu, C., Sun, F., et al. (2024). Unrestricted molecular motions enable mild photothermy for recurrence-resistant FLASH antitumor radiotherapy. *Bioact. Mater* 37, 299–312. doi:10.1016/j.bioactmat.2024.03.024

Shi, L., Zhu, M., Long, R., Wang, S., Wang, P., and Liu, Y. (2024a). Prussian blue nanoparticle-based pH-responsive self-assembly for enhanced photothermal and chemotherapy of tumors. *J. Photochem Photobiol. B* 256, 112938. doi:10.1016/j.jphotobiol.2024.112938

Shi, M., Paquette, B., Thippayamontri, T., Gendron, L., Guerin, B., and Sanche, L. (2016). Increased radiosensitivity of colorectal tumors with intra-tumoral injection of low dose of gold nanoparticles. *Int. J. Nanomedicine* 11, 5323–5333. doi:10.2147/IJN.S97541

Shin, S. M., Park, H. I., and Sung, A. Y. (2023). Correlation analysis of surface and physical properties of ophthalmic lenses containing nanoparticles. *Micromachines (Basel)* 14 (10), 1883. doi:10.3390/mi14101883

Shi, Y., Liao, J., Zhang, C., Wu, Q., Hu, S., Yang, T., et al. (2024b). Cascade-responsive size/charge bidirectional-tunable nanodelivery penetrates pancreatic tumor barriers. *Chem. Sci.* 15 (38), 15647–15658. doi:10.1039/d4sc04782f

Stefancikova, L., Lacombe, S., Salado, D., Porcel, E., Pagacova, E., Tillement, O., et al. (2016). Effect of gadolinium-based nanoparticles on nuclear DNA damage and repair in glioblastoma tumor cells. *J. Nanobiotechnology* 14 (1), 63. doi:10.1186/s12951-016-0215-8

Stergioula, A., Pantelis, E., Kontogeorgakos, V., Lazaris, A. C., and Agrogiannis, G. (2023). Understanding the role of radio-sensitizing nanoparticles in enhancing pathologic response in soft tissue sarcomas. *Cancers (Basel)* 15 (23), 5572. doi:10.3390/cancers15235572

Subiel, A., Ashmore, R., and Schettino, G. (2016). Standards and methodologies for characterizing radiobiological impact of high-Z nanoparticles. *Theranostics* 6 (10), 1651–1671. doi:10.7150/thno.15019

Sun, W., Luo, L., Feng, Y., Qiu, Y., Shi, C., Meng, S., et al. (2020). Gadolinium-rose bengal coordination polymer nanodots for MR-/Fluorescence-Image-Guided radiation and photodynamic therapy. *Adv. Mater* 32 (23), e2000377. doi:10.1002/adma.202000377

Tabatabaie, F., Franich, R., Feltis, B., and Geso, M. (2022). Oxidative damage to mitochondria enhanced by ionising radiation and gold nanoparticles in cancer cells. *Int. J. Mol. Sci.* 23 (13), 6887. doi:10.3390/ijms23136887

Taggart, L. E., Mcmahon, S. J., Currell, F. J., Prise, K. M., and Butterworth, K. T. (2014). The role of mitochondrial function in gold nanoparticle mediated radiosensitisation. *Cancer Nanotechnol.* 5 (1), 5. doi:10.1186/s12645-014-0005-7

Tan, H., Fu, S., Shen, L., Lin, Q., Li, W., Ran, Y., et al. (2025). Bioeliminable Pt@Bi(2)Se(3)-RGD nanoassembly for enhancing photoacoustic imaging-guided tumor immuno-radiotherapy by inducing apoptosis via the areg pathway. *Theranostics* 15 (7), 2720–2736. doi:10.7150/thno.106479

Teoh, M., Clark, C. H., Wood, K., Whitaker, S., and Nisbet, A. (2011). Volumetric modulated arc therapy: a review of current literature and clinical use in practice. *Br. J. Radiol.* 84 (1007), 967–996. doi:10.1259/bjr/22373346

Traneus, E., and Oden, J. (2019). Introducing proton track-end objectives in intensity modulated proton therapy optimization to reduce linear energy transfer and relative biological effectiveness in critical structures. *Int. J. Radiat. Oncol. Biol. Phys.* 103 (3), 747–757. doi:10.1016/j.ijrobp.2018.10.031

Tsai, C. Y., Ko, H. J., Huang, C. F., Lin, C. Y., Chiou, S. J., Su, Y. F., et al. (2021). Ionizing radiation induces resistant glioblastoma stem-like cells by promoting autophagy via the wnt/β-catenin pathway. *Life (Basel)* 11 (5), 451. doi:10.3390/life11050451

Tsai, S. W., Lo, C. Y., Yu, S. Y., Chen, F. H., Huang, H. C., Wang, L. K., et al. (2022). Gold nanoparticles enhancing generation of ROS for Cs-137 radiotherapy. *Nanoscale Res. Lett.* 17 (1), 123. doi:10.1186/s11671-022-03761-w

Tudda, A., Donzelli, E., Nicolini, G., Semperboni, S., Bossi, M., Cavaletti, G., et al. (2022). Breast radiotherapy with kilovoltage photons and gold nanoparticles as radiosensitizer: an *in vitro* study. *Med. Phys.* 49 (1), 568–578. doi:10.1002/mp.15348

Velten, C., and Tome, W. A. (2023). Reproducibility study of Monte Carlo simulations for nanoparticle dose enhancement and biological modeling of cell survival curves. *Biomed. Phys. Eng. Express* 9 (4), 045004. doi:10.1088/2057-1976/acd1f1

Verginadis, I. I., Citrin, D. E., Ky, B., Feigenberg, S. J., Georgakilas, A. G., Hill-Kayser, C. E., et al. (2025). Radiotherapy toxicities: mechanisms, management, and future directions. *Lancet* 405 (10475), 338–352. doi:10.1016/S0140-6736(24)02319-5

Wang, C., Jiang, Y., Li, X., and Hu, L. (2015). Thioglucose-bound gold nanoparticles increase the radiosensitivity of a triple-negative breast cancer cell line (MDA-MB-231). *Breast Cancer* 22 (4), 413–420. doi:10.1007/s12282-013-0496-9

Wang, D., Liao, Y., Zeng, H., Gu, C., Wang, X., Zhu, S., et al. (2024a). Manipulating radiation-sensitive Z-DNA conformation for enhanced radiotherapy. *Adv. Mater* 36 (29), e2313991. doi:10.1002/adma.202313991

Wang, J., Xin, Y., Chen, D., Zhang, N., Xue, Y., Liu, X., et al. (2025). Ultra-stable gold nanoparticles with tunable surface characteristics. *Angew. Chem. Int. Ed. Engl.*, e202507954. doi:10.1002/anie.202507954

Wang, Z., Ren, X., Li, Y., Qiu, L., Wang, D., Liu, A., et al. (2024b). Reactive oxygen species amplifier for apoptosis-ferroptosis mediated high-efficiency radiosensitization of tumors. *ACS Nano* 18 (14), 10288–10301. doi:10.1021/acsnano.4c01625

Wu, J., Chen, K., Pan, J., Li, D., Ma, Y., and Li, N. (2024). Ultrasensitive SERS profiling of intracellular hydrogen peroxide release based on enzymatic amplification and silent-region Raman reporter. *Anal. Chem.* 96 (50), 19981–19987. doi:10.1021/acs.analchem.4c04544

Xiao, L., Chen, B., Wang, W., Tian, T., Qian, H., Li, X., et al. (2023). Multifunctional Au@AgBiS(2) nanoparticles as high-efficiency radiosensitizers to induce pyroptosis for cancer radioimmunotherapy. *Adv. Sci. (Weinh)* 10 (30), e2302141. doi:10.1002/advs.202302141

Xu, M., Xu, C., Qiu, Y., Feng, Y., Shi, Q., Liu, Y., et al. (2024). Zinc-based radioenhancers to activate tumor radioimmunotherapy by PD-L1 and cGAS-STING pathway. *J. Nanobiotechnology* 22 (1), 782. doi:10.1186/s12951-024-02999-z

Xu, X., Wu, J., Dai, Z., Hu, R., Xie, Y., and Wang, L. (2022). Monte Carlo simulation of physical dose enhancement in core-shell magnetic gold nanoparticles with TOPAS. *Front. Oncol.* 12, 992358. doi:10.3389/fonc.2022.992358

Yadav, P., Bandyopadhyay, A., and Sarkar, K. (2024). Enhancement of gold-curcumin nanoparticle mediated radiation response for improved therapy in cervical cancer: a computational approach and predictive pathway analysis. *Discov. Nano* 19 (1), 153. doi:10.1186/s11671-024-04104-7

Yang, D., Youden, B., Yu, N., Carrier, A. J., Jiang, R., Servos, M. R., et al. (2025). Surface-enhanced Raman spectroscopy for the detection of reactive oxygen species. *ACS Nano* 19 (2), 2013–2028. doi:10.1021/acsnano.4c15509

Yang, X., Salado-Leza, D., Porcel, E., Gonzalez-Vargas, C. R., Savina, F., Dragoe, D., et al. (2020). A facile one-pot synthesis of versatile PEGylated platinum nanoflowers and their application in radiation therapy. *Int. J. Mol. Sci.* 21 (5), 1619. doi:10.3390/ijms21051619

Yang, X., Tran, V. L., Remita, H., Savina, F., Denis, C., Kereselidze, D., et al. (2022). Pharmacokinetics derived from PET imaging of inspiring radio-enhancer platinum nanoparticles. *Nanomedicine* 46, 102603. doi:10.1016/j.nano.2022.102603

Yan, S., Ngoma, T. A., Ngwa, W., and Bortfeld, T. R. (2023). Global democratisation of proton radiotherapy. *Lancet Oncol.* 24 (6), e245–e254. doi:10.1016/S1470-2045(23)00184-5

Yu, C. N. Y. W. B. Y. X. H. Q. S. T., Yang, W., Bao, Y., Xu, H., Qin, S., and Tu, Y. (2015). BSA capped Au nanoparticle as an efficient sensitizer for glioblastoma tumor radiation therapy. *R. Soc. Chem. Adv.* 5 (51), 40514–40520. doi:10.1039/c5ra04013b

Yuan, K., Zhang, C., Pan, X., Hu, B., Zhang, J., and Yang, G. (2024). Immunomodulatory metal-based biomaterials for cancer immunotherapy. *J. Control Release* 375, 249–268. doi:10.1016/j.jconrel.2024.09.008

Zhang, X. D., Wu, D., Shen, X., Chen, J., Sun, Y. M., Liu, P. X., et al. (2012). Size-dependent radiosensitization of PEG-coated gold nanoparticles for cancer radiation therapy. *Biomaterials* 33 (27), 6408–6419. doi:10.1016/j.biomaterials.2012.05.047

Zhang, J., Rinne, S. S., Yin, W., Leitao, C. D., Bjorklund, E., Abouzayed, A., et al. (2024). Affibody-drug conjugates targeting the human epidermal growth factor receptor-3 demonstrate therapeutic efficacy in mice bearing low expressing xenografts. *ACS Pharmacol. Transl. Sci.* 7 (10), 3228–3240. doi:10.1021/acsptsci.4c00402

Zhang, P., Yu, B., Jin, X., Zhao, T., Ye, F., Liu, X., et al. (2021). Therapeutic efficacy of carbon ion irradiation enhanced by 11-MUA-capped gold nanoparticles: an *in vitro* and *in vivo* study. *Int. J. Nanomedicine* 16, 4661–4674. doi:10.2147/IJN.S313678

Zhang, R., Chen, M., Zhou, H., Liu, Y., Wang, Y., Chen, C., et al. (2025). Eliminating radioresistance with a magnetic ion-generator by simultaneously augmenting DNA damage and diminishing immunosuppression. *Adv. Mater* 37, e2406378. doi:10.1002/adma.202406378

Zhang, X., Cai, X., and Yan, C. (2023). Opportunities and challenges in combining immunotherapy and radiotherapy in esophageal cancer. *J. Cancer Res. Clin. Oncol.* 149 (20), 18253–18270. doi:10.1007/s00432-023-05499-z

Zhao, J., Li, D., Ma, J., Yang, H., Chen, W., Cao, Y., et al. (2021). Increasing the accumulation of aptamer AS1411 and verapamil conjugated silver nanoparticles in tumor cells to enhance the radiosensitivity of glioma. *Nanotechnology* 32 (14), 145102. doi:10.1088/1361-6528/abd20a

Zheng, Y., and Sanche, L. (2023). Mechanisms of nanoscale radiation enhancement by metal nanoparticles: role of low energy electrons. *Int. J. Mol. Sci.* 24 (5), 4697. doi:10.3390/ijms24054697

Zhen, W., Weichselbaum, R. R., and Lin, W. (2023). Nanoparticle-mediated radiotherapy remodels the tumor microenvironment to enhance antitumor efficacy. *Adv. Mater* 35 (21), e2206370. doi:10.1002/adma.202206370

Zhu, H., Zhang, Z., Jiang, R., Xu, L., Yang, X., Chen, J., et al. (2025a). MXene-based nanosheet for enhanced glioma therapy via photonic hyperthermia to boost the abscopal effect of radioimmunotherapy. *J. Nanobiotechnology* 23 (1), 203. doi:10.1186/s12951-025-03288-z

Zhu, X., Qiu, C. J., Cao, J. J., Duosiken, D., Zhang, Y., Pei, B. G., et al. (2025b). Radiosensitization of rare-earth nanoparticles based on the consistency between its K-edge and the X-ray bremsstrahlung peak. *J. Funct. Biomater.* 16 (2), 41. doi:10.3390/jfb16020041

Zou, Y. M., Li, R. T., Yu, L., Huang, T., Peng, J., Meng, W., et al. (2023). Reprogramming of the tumor microenvironment using a PCN-224@IrNCs/D-Arg nanoplatform for the synergistic PDT, NO, and radiosensitization therapy of breast cancer and improving anti-tumor immunity. *Nanoscale* 15 (25), 10715–10729. doi:10.1039/d3nr01050c

Zou, Y., Xu, H., Wu, X., Liu, X., and Zhao, J. (2024). Enhancing radiotherapy sensitivity in prostate cancer with lentinan-functionalized selenium nanoparticles: mechanistic insights and therapeutic potential. *Pharmaceutics* 16 (9), 1230. doi:10.3390/pharmaceutics16091230